Sedimentary Geology 364 (2018) 1–13

Contents lists available at ScienceDirect

Sedimentary Geology

journal homepage: www.elsevier.com/locate/sedgeo

New aragonite $^{87}Sr/^{86}Sr$ records of Mesozoic ammonoids and approach to the problem of N, O, C and Sr isotope cycles in the evolution of the Earth

Yuri D. Zakharov [a,*], Sergei I. Dril [b], Yasunari Shigeta [c], Alexander M. Popov [a], Eugenij Y. Baraboshkin [d], Irina A. Michailova [d], Peter P. Safronov [a]

[a] Far Eastern Geological Institute, Russian Academy of Sciences (Far Eastern Branch), Stoletiya Prospect 159, Vladivostok 690022, Russia
[b] Institute of Geochemistry, Russian Academy of Sciences (Siberian Branch), Favorsky Street 1a, Irkutsk 664033, Russia
[c] National Museum of Nature and Science, 4-1-1 Amakubo, Tsukuba, Ibaraki 305-0005, Japan
[d] Moscow State University, Leninskiye Gory MGU 1, Moscow 11991, Russia

ARTICLE INFO

Article history:
Received 2 October 2017
Received in revised form 21 November 2017
Accepted 23 November 2017
Available online 28 November 2017

Editor: Dr. B. Jones

Keywords:
Mesozoic
Ammonoids
Sr, O, C, N isotope cycles
Eurasia
America

ABSTRACT

New Sr isotope data from well-preserved aragonite ammonoid shell material from the Mesozoic are compared with that from a living *Nautilus* shell. The prominent negative Sr isotope excursions known from the Middle Permian, Jurassic and Cretaceous probably have their origins in intensive plate tectonic activity, followed by enhanced hydrothermal activity at the mid-ocean ridges (mantle volcanism) which supplied low radiogenic Sr to seawater. The maximum positive (radiogenic) shift in the lower Mesozoic Sr isotope curve (Lower Triassic peak) was likely caused by a significant expansion of dry land surfaces (Dabie-Sulu Triassic orogeny) and their intensive silicate weathering in conditions of extreme warming and aridity in the very end of the Smithian, followed by warm and humid conditions in the late Spathian, which apparently resulted in a significant oceanic input of radiogenic Sr through riverine flux. The comparatively high $^{87}Sr/^{86}Sr$ ratio obtained from the living *Nautilus* shell is probably a function of both the Alpine orogeny, which was accompanied by significant continental weathering and input of radiogenic Sr to the oceans, and the weakening of mantle volcanism.

1. Introduction

Over the past four decades vast data on Phanerozoic Sr-isotope stratigraphy have been compiled from calcitic and apatite fossil material and whole-rock samples (e.g., Veizer and Compston, 1974; Brass, 1976; Burke et al., 1982; Hess et al., 1986; Koepnick et al., 1990; Clements et al., 1993; McArthur et al., 1993, 2000, 2004, 2012, 2016; Denison et al., 1994, 2003; McArthur, 1994; Jones et al., 1994; Jenkyns et al., 1995, 2002; Martin and MacDougell, 1995; Veizer et al., 1999; Zachos et al., 1999; Jones and Jenkyns, 2001; Korte et al., 2003, 2004, 2006; Van Geldern et al., 2006; Wotte et al., 2007; Prokoph et al., 2008; Wierzbowski, 2013; Madhavaraju et al., 2015). However, only a few aragonite-preserved fossils, originating mostly from the Campanian and upper Maastrichtian of North America (e.g., Cochran et al., 2003, 2016) and the lower Albian of Madagascar (Zakharov et al., 2016) have been used for this purpose. The benefit of aragonitic fossils in isotope studies lies in their absence of significant diagenetic alteration.

This paper focuses on some Mesozoic Sr isotope oscillations, derived from the study of well-preserved, aragonitic cephalopod shells. We also present oxygen and carbon isotope data from ammonoids and other fossils, and some paleoenvironmental reconstructions.

2. Materials and methods

Material for Sr isotope investigation includes ammonoid shells from the lower and upper Olenekian and mid Anisian of Arctic Siberia, the lower Toarcian of Western Switzerland, the upper Callovian and lower Aptian of the Russian Platform, the upper Santonian and lower Campanian of North America, and finally a shell of living *Nautilus pompilius* Lenne from the Philippines (Fig. 1). Lower Toarcian mollusc shells from Western Switzerland, as well as some fossils from the lower Bathonian and lower Callovian of Central Switzerland, upper Hauterivian of Argentina, and lower Barremian of the Alps were also utilized for O and C isotope investigations.

The following criteria were used to determine diagenetic alteration: (1) hand-sample visual indications; (2) percentage of aragonite in mollusc shells, which were originally represented by 100% aragonite; (3) presence or lack of diagenetic admixture, determined by X-ray diffraction analysis; (4) the degree of integrity of shell microstructure,

* Corresponding author.
E-mail addresses: yurizakh@mail.ru (Y.D. Zakharov), sdril@igc.irk.ru (S.I. Dril), shigeta@kahaku.go.jp (Y. Shigeta), popov_alexander@list.ru (A.M. Popov), ejbaraboshkin@mail.ru (E.Y. Baraboshkin), tamara_soboleva@mail.ru (I.A. Michailova), psafronov@mail.ru (P.P. Safronov).

https://doi.org/10.1016/j.sedgeo.2017.11.011
0037-0738/

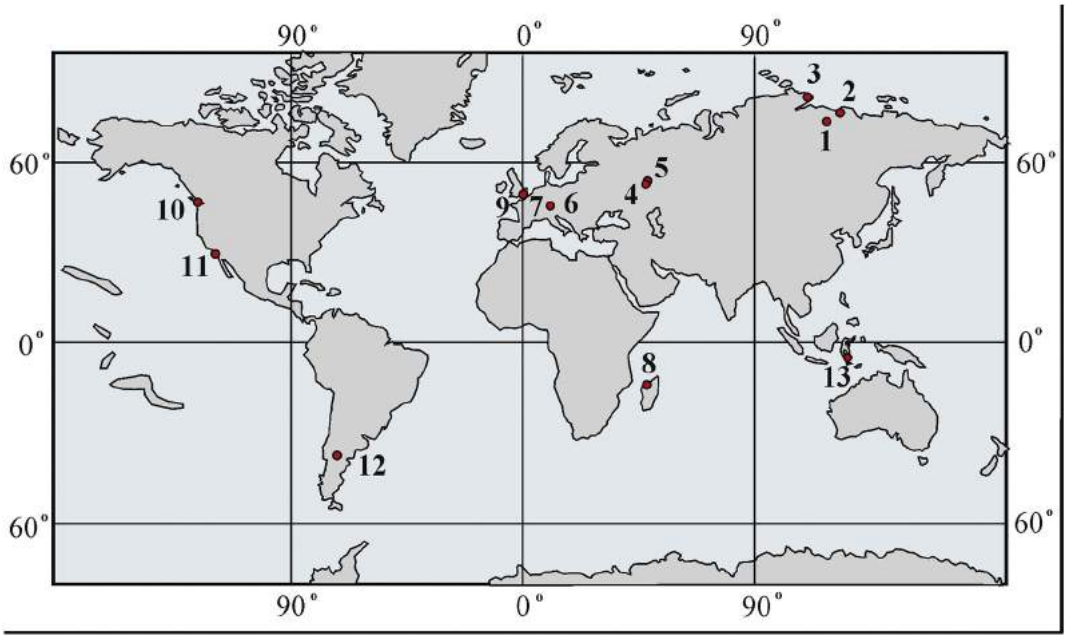

Fig. 1. Location of investigated areas: 1, Buur River, Arctic Siberia (Induan–Olenekian boundary beds; 2, Mengilyakh Creek, Olenek River (uppermost Olenekian); 3, Keshin Creek, Taimyr (mid Anisian); 4, Ryazan area, Russian Platform (upper Callovian); 5, Ulyanovsk area, Russian Platform (lower Aptian); 6, Teysachaux mountain, Western Switzerland (lower Toarcian); 7, the village of Anwill, Northern Switzerland (Bathonian–Callovian boundary); 8, Madagascar (lower Albian); 9. Dorset, South West Englang (uppermost Berriassian); 10, Vancouver Island, British Columbia (upper Santonian); 11, Butte Creek, California (lower Campanian); 12, Patagonia (upper Hauterivian); 13, Bohol Island area, Philippines (living *Nautilus pompilius* Linne).

determined under a scanning electron microscope (SEM). We have recognized four stages of diagenetic alteration in aragonitic mollusc shells (Zakharov et al., 1975, 2016).

X-ray powder analyses were carried out at the Analytical Centre (FEGI) in Vladivostok using a desktop X-ray diffractometer MiniFlex II (Rigaku Firm). SEM and X-ray studies of selected Mesozoic fossils suggest that most of them retain their original shell microstructure, and thus their original Sr, C and O isotope compositions. X-ray diffraction analysis reveals the lack of secondary admixtures, including α-SiO_2, in most samples from this area, and 75–100% aragonitic composition of most of our selected ammonoids, and some bivalve shells.

O and C isotope measurements at the Stable Isotope Laboratory (*FEGI FEB RAN, Vladivostok*). Oxygen and carbon isotope measurements were carried out using a Finnigan MAT-252 (Analytical Centre, FEGI, Vladivostok). The laboratory gas standard used in the O and C isotope measurements was calibrated relatively to NBS-19 $\delta^{13}C = 1.93‰$ and $\delta^{18}O = -2.20‰$ (Coplen et al., 1983). Reproducibility of replicate standards was always better than 0.1‰.

The following equation was used for palaeotemperature calculation (Grossman and Ku, 1986): $T\ (C) = 20.6–4.34\ (\delta^{18}O_{aragonite} - \delta w)$.

In this equation T (C) is the ambient temperature; $\delta^{18}O_{aragonite}$ is the measured oxygen-isotope value of aragonite (versus VPDB), and δw (‰) is the ambient water isotope ratio (versus VSMOW). A δw of −1.0‰ is often assumed to be appropriate for an ice-free world (e.g., Shackleton and Kennet, 1975; Hudson and Anderson, 1989; Huber et al., 2002; Pirrie and Marshall, 1990; Price and Hart, 2002; Lukeneder et al., 2010). It is known that there are definitely ice and ice-free times during Mesozoic (Price and Passey, 2013; Veizer and Prokoph, 2015), but intervals investigated in this study correspond to ice-free times. However, the isotopic composition of Cretaceous seawater may have varied considerably due to freshwater input and/or evaporation.

Sr isotope measurements at the Laboratory of Isotope Geochemistry (*IG SB RAS, Irkutsk*). Laboratory methods for the Sr isotope analysis followed instrumental and operating specifications as discussed in Degryse and Schneider (2008). Material for our Sr isotope investigation, taken from well preserved cephalopod shells that still exist in their original aragonitic mineralogy, was obtained by chemical preparation of straight Sr fractions, using ion-exchange polymers BioRad AG 50W*8, 200–400 mesh and BioRad AG 50*12, 200–400 mesh (Collective Enjoyment Center of Isotope Geochemical Investigation, Institute of Geochemistry of Russian Academy of Sciences, Siberian Branch, Irkutsk).

>50 ng (nanogram) of each sample were loaded onto rhenium filaments (cathode) and analyzed for $^{87}Sr/^{86}Sr$ on a Finnigan MAT-262 seven-collector (Collective Joint Center of Geodynamic and Geochronology, Institute of Earth Core, Russian Academy of Sciences, Siberian Branch, Irkutsk) using the multi-dynamic routines that include a correction for isobaric interference from ^{87}Rb ($^{87}Rb/^{85}Rb = 0.386$). The rhenium cathode was previously covered by an activator, prepared on the basis of Ta_2O_5. The ^{88}Sr ion current was usually been equal to $2–3 * 10^{(-11)}$ A. Data have been normalized to a value of 8.37521 for $^{88}Sr/^{86}Sr$.

$^{87}Sr/^{86}Sr$ measurements were made using the following most common standards: (1) NBS-987 (known earlier as SRM987); and (2) BCR-2. The $^{87}Sr/^{86}Sr$ values for these standards are (1) 0.710249 ± 8 (2 SD, n = 12); and (2) 0.705011 ± 14 (2 SD, n = 7) respectively, where SD is standard deviation and n is number of measurements. External precision (2σ) is typically in the range of ±0.00001 to ±0.00003 (Banner, 2004).

3. $^{87}Sr/^{86}Sr$, $\delta^{18}O$ and $\delta^{13}C$ records

3.1. Cretaceous

Previously, Sr isotope data for the Cretaceous has been obtained from aragonite-preserved lower Albian *Eotetragonites*, *Desmoceras*, *Cleoniceras*, and *Douvilleiceras* shells from Madagascar ($^{87}Sr/^{86}Sr$ = 0.707241–0.707276; Zakharov et al., 2016) and upper Maastrichtian *Sphenodiscus*, *Hoploscaphites* and *Discoscaphites* shells from North America ($^{87}Sr/^{86}Sr = 0.707699–0.707795$; Cochran et al., 2003). We now add to this data with material from the Russian Platform and from North America.

Ulyanovsk area, *Russian Platform* (*middle lower Aptian*). Sr isotopes were analyzed from two *Deshayesites volgensis* Sazonova shells (Fig. 2) from this locality. Both shells were collected from calcareous-marl concretions in a 3.8–4.0 m thick layer of black bituminous shale (OAE 1a, also known as the Selli Event) of the Volgensis-Schilovkensis Zone (Gavrilov et al., 2002; Zakharov et al., 2013a).

Shell 45/96 of *Deshayesites volgensis*, a middle-sized and silvery-white (D = 160 mm; 84–100% aragonite) specimen, is characterised by a comparatively low Sr isotope ratio ($^{87}Sr/^{86}Sr = 0.707382$) at H = 55 mm (Table S1). $\delta^{18}O$ and δ13C values in this shell fluctuate from −2.59 to −2.24‰ and from −3.8 to −1.97‰, respectively (Zakharov et al., 2013a). The $\delta^{18}O$ values suggest comparatively high paleotemperatures (25.1–26.8 °C).

Another investigated shell of *Deshayesites volgensis* (50/96), middle-sized and silvery-white (D = 61.0 mm; 95–100% aragonite), is also characterised by a comparatively low Sr-isotope ratio ($^{87}Sr/^{86}Sr = 0.707333$) at H = 27.5 mm (Table S1). $\delta^{18}O$ and $\delta^{13}C$ values in this shell vary between −3.6 to −2.6‰ and −2.8 to −0.6‰, respectively. The $\delta^{18}O$ values of this shell indicate somewhat higher palaeotemperatures (26.7–30.8 °C).

Vancouver, *British Columbia* (upper Santonian Haslam Fm.; Ward et al., 2012). We have analyzed the Sr isotope composition of a mid-sized, cream-colored ammonoid *Pseudoschloenbachia umbulazi* (Baily) shell (shell fragment PS(2); 89–100% aragonite), found in a calcareous-marl concretion of the Haslam Formation (Yokoyamai Zone, up to 150 m) in the Brannan Lake area, Vancouver Island. A

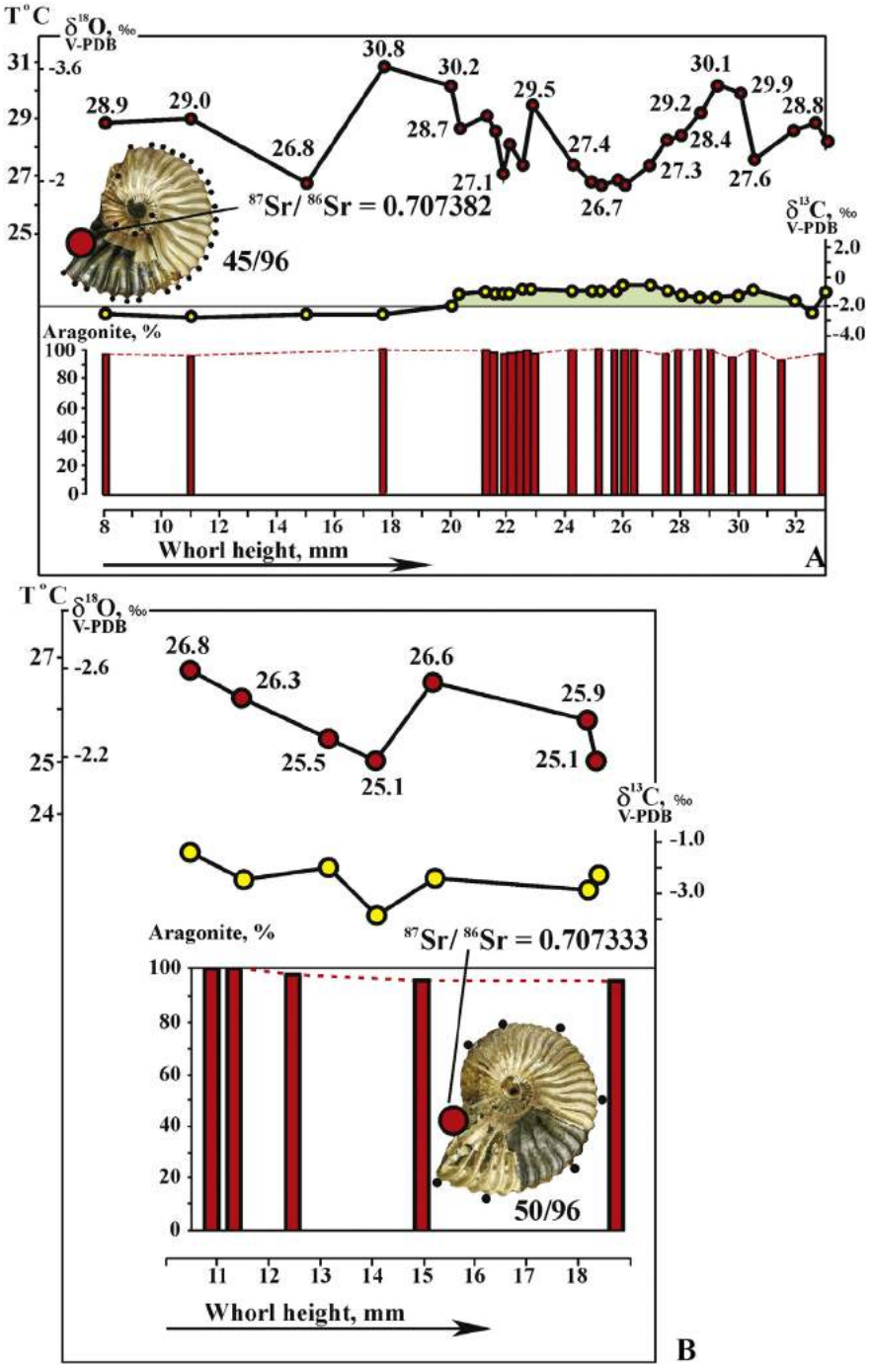

Fig. 2. Lower Aptian Volgensis-Shilovkensis Zone; Russian Platform, Ulyanovsk area: Sr-C-, O-isotope and palaeotemperature data. A, *Deshayesites volgensis* Sasonova, no. 45/96, Ulyanovsk environs; B, *D. volgensis* Sasonova, no. 50/96, Kraushi.

Table 1
Carbon and oxygen isotope analyses of some brachiopod and mollusc shells from Jurassic-Cretaceous deposits of Western Europe and South America (H, height, L, length).

Sample	Shell	Species (locality, stage, zone, formation)	Location (H or L in mm)	Diagenetic alterations				$\delta^{13}C$ (VPDB), ‰	$\delta^{18}O$ (VPDB), ‰	T, °C
				Diagenetic stage	Aragonite (calcite), %	Admixture (e.g., α-SiO_2)	Colour			
HS2–1	HS2	*Hildaites serpentinum* Buckman (Western Switzerland, western slope of the Mount Teysachaux; lower Toarcian; Y.D. Zakharov's coll.)	H = 22?	2nd	83 (17)	No	Cream	0.32	−2.44	25.98
HS2–2	Same shell	*Hildaites serpentinum*	H = 21	2nd	76 (24)	α-SiO_2 (traces)	Cream	0.37	–-2.77	27.4
HS2–3	Same shell	*Hildaites serpentinum*	H = 20.5	2nd	81 (19)	No	Cream	0.70	−2.40	25.81
HS2–4	Same shell	*Hildaites serpentinum*	H = 20	2nd	79 (21)	α-SiO_2 (traces)	Cream	0.74	−2.57	26.55
HS2–5	Same shell	*Hildaites serpentinum*	H = 19.5	2nd	82 (18)	No	Cream	0.89	−2.43	25.94
HS2–6	Same shell	*Hildaites serpentinum*	H = 19.2	2nd	82 (18)	α-SiO_2 (traces)	Cream	0.85	−2.64	26.85
HS2–7	Same shell	*Hildaites serpentinum*	H = 19.0	2nd	81 (19)	No	Cream	0.89	−2.48	26.16
HS2–8	Same shell	*Hildaites serpentinum*	H = 18.5	2nd	75 (25)	α-SiO_2 (traces)	Cream	0.84	−2.69	29.08
HS2–9	Same shell	*Hildaites serpentinum*	H = 18.0	2nd	77 (23)	α-SiO_2 (traces)	Cream	0.60	−2.75	27.33
HS2–10	Same shell	*Hildaites serpentinum*	H = 15.0	2nd	76 (24)	α-SiO_2 (traces)	Cream	−0.93	−3.41	22.49
HS2–11	Same shell	*Hildaites serpentinum*	H = 14.5	3rd	67 (33)	α-SiO_2 (traces)	Cream	−0.01	−3.58	30.93
HS2–12	Same shell	*Hildaites serpentinum*	H = 12.0	2nd	82 (18)	α-SiO_2 (traces)	Cream	0.02	−2.91	28.02
HS2–13	Same shell	*Hildaites serpentinum*	H = 10.0	–	–	–	Cream	0.05	−3.17	30.19
HS2–14	Same shell	*Hildaites serpentinum*	H = 9.5	2nd	78 (22)	α-SiO_2 (traces)	Cream	−0.13	−3.06	28.68
HS2–15	Same shell	*Hildaites serpentinum*	H = 9.0	–	–	–	Cream	−0.04	−3.07	27.75
HS2–16	Same shell	*Hildaites serpentinum*	H = 7.5	2nd	80 (20)	α-SiO_2 (much)	Cream	−0.18	−3.11	28.89
HS2–17	Same shell	*Hildaites serpentinum*	H = 7.0		60	α-SiO_2 (traces)	Cream	−0.21	−3.31	29.79
HS2–18	Same shell	*Hildaites serpentinum*	H = 5.0	–	–	–	Cream	−0.12	−3.52	30.67
HS2–19	Same shell	*Hildaites serpentinum*	H = 4.0	–	–	–	Cream	−0.16	−3.68	31.36
HS32	HS32	*Hildaites serpentinum* (same locality)	H = 7.0	–	–	–	Cream	0.47	−3.20	29.28
HS7	HS7	Phylloceratidae? gen. et sp. indet. (same locality)	H = 8.0	2nd	81	α-SiO_2 (traces)	Cream	−0.24	−2.70	27.11
HS10	HS10	Phylloceratidae? gen. et sp. indet. (same locality)	H = 9.0	2nd	84	α-SiO_2 (traces)	Cream	−0.93	−1.63	22.47
HS15	HS15	Phylloceratidae? gen. et sp. indet. (same locality)	H = 8.9	2nd	79	α-SiO_2 (traces)	Cream	−0.04	−3.82	31.97
HS29	HS29	Phylloceratidae? gen. et sp. indet. (same locality)	H = 15.0	–	–	–	Cream	0.46	−2.72	27.20
HS31	HS31	Phylloceratidae? gen. et sp. indet. (same locality)	H = 5.1	2nd	74	α-SiO_2 (traces)	Cream	0.31	−3.13	28.98
HS33	HS33	Phylloceratidae? gen. et sp. indet. (same locality)	H > 14.0	2nd	92	α-SiO_2 (traces)	Cream	−0.99	−2.23	25.07
HS 34	HS34	Phylloceratidae? gen. et sp. indet. (same locality)	H = 11.0	2nd	71	α-SiO_2 (traces)	Cream	−1.33	−3.57	30.89
HS16	HS16	*Unicardium bollense* Bassi (same locality)	H = 18.0	2nd	81	α-SiO_2 (traces)	Cream	−0.18	−2.95	28.20
HS3	HS3	*Unicardium bollense* (same locality)	H = 13.0	–	–	–	Cream	−0.97	−3.07	28.72
HS18	HS18	*Unicardium bollense* (same locality)	H = 14	2nd	80	α-SiO_2 (traces)	Cream	0.05	−3.12	28.93
HS19	HS19	*Unicardium bollense* (same locality)	H = 17	2nd	71	α-SiO_2 (traces)	Cream	−0.05	−3.79	31.84
HS11	HS11	*Unicardium bollense* (same locality)	H > 8.0	–	–	–	Cream	0.11	−3.20	29.28
HS27	HS27	*Unicardium bollense* (fragment; same locality)	–	2nd	85	α-SiO_2 (traces)	Cream	−0.54	−2.48	26.16
HS30	HS30	*Unicardium bollense* (same locality)	H = 8.0	2nd	86	α-SiO_2 (traces)	Cream	0.22	−4.62	35.44
HS12	HS12	*Unicardium bollense* (same locality)	H = 10.0	–	–	–	Cream	1.83	−2.81	27.59
HS13	HS13	*Solemya voltzi* Roemer (same locality)	H = 7.0	1st	95	α-SiO_2 (traces)	Cream	1.65	−2.27	35.24
HS4	HS4	*Solemya voltzi* Roemer (same locality)	H = 6.0	2nd	80	(Trace)	Cream	1.0	−2.42	25.89
HS14	HS14	*Pseudomytiloides*? sp. (same locality)	H > 20.0	2nd	93	α-SiO_2 (traces)	Cream	1.25	−5.13	37.66
HS6	HS6	*Pseudomytiloides dubius* Sowerby (*same locality*)	H = 14.5	2nd	87 (13)	α-SiO_2 (traces)	Cream	2.15	−5.36	38.67

Table 1 (*continued*)

Sample	Shell	Species (locality, stage, zone, formation)	Location (H or L in mm)	Diagenetic alterations				$\delta^{13}C$ (VPDB), ‰	$\delta^{18}O$ (VPDB), ‰	T, °C
				Diagenetic stage	Aragonite (calcite), %	Admixture (e.g., α-SiO_2)	Colour			
Bs-1	Bs-1	Oyster bivalve (Switzerland, Auenstein quarry; upper *Bajocian*, *Stein Fm.; Y.D. Zakharov's coll.*)	H = 9	–	0 (100)	No	White	2.85	−1.56	16.58
Bs-2	Bs-2	Oyster bivalve (same locality and same formation)	H = 20	–	0 (100)	No	White	3.17	−2.31	21.66
Bt-1	Bt-1	Rhynchonellid brachiopod (Switzerland, Auenstein quarry; lower Bathonian, Klingnau Fm.; Y.D. Zakharov's coll.)	L = 21	–	0 (100)	No	White	3.11	−0.09	12.35
Bt-2	Bt-2	Rhynchonellid brachiopod (same locality, same formation)	L = 21.5	–	0 (100)	No	White	2.08	−2.88	24.28
C-1	C-1	Terebratulid brachiopods (three shells) (Switzerland, Anwil; lowermost Callovian, Anwil-Bank; Y.D. Zakharov's coll.)	L = 6–8	–	0 (100)	No	Silvery-white	0.02	−1.38	17.59
C-2	C-2	Terebratulid brachiopod (same locality)	L = 17	–	0 (100)	No	Silvery-white	1.78	−0.97	15.88
C-4-1	C-4	Oyster bivalve (same locality)	L = 15	–	0 (100)	No	Silvery-white	2.18	−0.61	14.41
C-4-2	Same shell	Oyster bivalve (same locality)	L = 24	–	0 (100)	No	Silvery-white	2.65	−0.53	14.00
C-4-3	Same shell	Oyster bivalve (same locality)	L = 35	–	0 (100)	No	Silvery-white	2.38	−041	13.61
C-4-4	Same shell	Oyster bivalve (same locality)	L = 45	–	0 (100)	No	Silvery-white	2.54	−0.62	14.45
C-4-5	Same shell	Oyster bivalve (same locality)	L-53	–	0 (100	No	Silvery-white	1.87	−1.31	17.30
Ht-2	Ht-2	Undetermined bivalve shell, fragment (Patagonia; upper *Hauterivian*, *Riccardii Zone*, *Agrio Fm.; Y.D. Zakharov's coll.*)	H > 40	–	0 (100)	No	White	1.57	−2.06	20.55
Br-1	Br-1	*Exogyra* sp. (Alps, Pillar 2 area, *Locality Tierwis; lower Barremian*, *Tierwis Fm.*, *Altmann Member; Y.D. Zakharov's coll.*)	H > 100	–	0 (100)	No	Light grey	1.82	−1.56	18.36

sample for Sr isotope analysis (Ps(2)-11) was taken from shell fragments at H = 38.5 mm, which is characterised by comparatively low Sr-isotope ratio ($^{87}Sr/^{86}Sr$ = 0.707281; Table S1).

Earlier published results (Zakharov et al., 2013b) show that $\delta^{18}O$ and $\delta^{13}C$ values in this shell vary between −3.1 to −2.6‰ and from −1.3 to −2.3‰, respectively. The $\delta^{18}O$ data indicates comparatively high paleotemperatures (26.6–28.8 °C).

California (lower Campanian Chico Fm.; Ward et al., 2012). A fragment of middle-sized, silvery-cream *Submortoniceras* sp. shell, specimen Cal-2 (100% aragonite) from the Chico Formation of the Butte Creek area, California (Chicoensis Zone) was used for Sr isotope investigation. This shell is also characterised by a comparatively low Sr-isotope ratio ($^{87}Sr/^{86}Sr$ = 0.707198; Table S1). $\delta^{18}O$ and $\delta^{13}C$ values vary between −2.0 to −1.9‰ and 1.0 to 1.2‰, respectively (Zakharov et al., 2006b). The $\delta^{18}O$ values in this shell fragment indicate comparatively high paleotemperatures (23.9–24.3 °C).

Additional original O and C isotope data obtained from some Lower-Middle Jurassic and Early Cretaceous fossils (51 samples) from western Switzerland (lower Bathonian Klingneu Fm.; Hostettler, 2014), northern Switzerland (uppermost Bathonian–lowermost Callovian Anwil bed; Etter, 2014b), Santis–massif, Switzerland Alps (lower Barremian Tierwis Fm.; Kürsteiner, 2014) and west-central Argentina (upper Hauterivian Agrio Fm.; Lazo et al., 2014) are given in Table 1.

3.2. Other intervals investigated

3.2.1. Triassic (Olenekian–Anisian)

Early and Middle Triassic aragonite-preserved ammonoids are known only from Arctic Siberia (e.g., Mojsisovics, 1886; Zakharov et al., 1975, 1987, 1999a; Zakharov, 1978). We have investigated the Sr isotope composition of Triassic ammonoids from three localities in Arctic Siberia: (1) Buur River (Olenek River basin); (2) Mengilyakh Creek (right bank of the lower reaches of the Olenek River); and (3) Keshin Creek, Tsvetkov Cape (eastern Taimyr).

Buur River (*lowermost Olenekian*). A large *Hedenstroemia hedenstroemi* (Keyserling) shell, specimen 890/4–5 (up to 120 mm in diameter) was found in a calcareous-marl concretion from lowermost Olenekian mudstone of the Hedenstroemi Zone of this locality. A sample for Sr-isotope analysis was taken from the best-preserved cream-colored area (98% aragonite) of its outer whorl, consisting of three layers: external prismatic, nacreous and inner prismatic (Zakharov et al., 1987). A comparatively high Sr-isotope ratio ($^{87}Sr/^{86}Sr$ = 0.708043; Table S1) was determined from this sample. According to our previous study (Zakharov et al., 1999a), this area is characterised by $\delta^{18}O$ of −4‰ and $\delta^{13}C$ of −0.3‰ at H = 98 mm.

Mengilyakh Creek (*uppermost Olenekian*). A medium-sized specimen of *Boreomeekoceras keyserlingi* (Mojsisovics), specimen 45/802 (D = 76.0 mm) was found in a calcareous-marl concretion from uppermost Olenekian mudstone of the Spiniplicatus Zone (Fig. 3). The investigated cream-colored area (87% aragonite at H = 27.0 mm) records a very high Sr-isotope ratio ($^{87}Sr/^{86}Sr$ = 0.709041; Table S1), similar to that of our living *Nautilus pompilius* Linne shell from the Philippines. The investigated *Boreomeekoceras keyserlingi* shell is characterised by lower $\delta^{18}O$ and $\delta^{13}C$ values in comparison with those obtained from the *Hedenstroemia hedenstroemi* shell: −6.0‰ and −3.3‰, respectively (Zakharov et al., 1999a).

Keshin Creek (*middle Anisian*). A small, cream-colored *Arctohungarites* sp. shell, specimen 4/816 (up to 30 mm in diameter; 88% aragonite) was collected in a calcareous-marl concretion from middle Anisian mudstone (likely from the Kharaulakhensis Zone). The calculated Sr-isotope ratio ($^{87}Sr/^{86}Sr$ = 0.707744; Table S1) in this shell is also comparatively high. This shell is characterised by $\delta^{18}O$ and $\delta^{13}C$ values of −4.1 and −2.3‰ at H = 15.8 mm, respectively (Zakharov et al., 1999a).

Following Hallam (1969) and Zakharov et al. (1975), we suggest that the comparatively low $\delta^{18}O$ values of aragonite preserved in our Olenekian and Anisian ammonoid shells from Arctic Siberia is a function of the environment that these ammonoids inhabited being within the Boreal realm under reduced salinity conditions. Our previous calculations, applying a water correction for approximate computation of palaeotemperatures in the shallow-water Olenekian-Anisian sea of Arctic Siberia, give mean values for early and late Olenekian and Anisian of ?8.8, ?16.3 and ?15.4 °C, respectively (Zakharov et al., 1999a).

3.2.2. Jurassic

We have investigated the Sr isotope composition of Jurassic ammonoids from the following localities in Europe: (1) Western Switzerland in the Pre-Alps area; and (2) the Ryazan area on the Russian Platform.

Western slope of the Mount Teysachaux, Switzerland (*lower Toarcian Levisoni to Falciferum zones*). The lower Toarcian ammonoids *Hildaites serpentinum* Buckman (Fig. 3), *Harpoceras falciferum* Sowerby and Phylloceratidae? gen. et sp. indet. are well known from the 10 m thick organic-rich "*Posidonia* Shale", or "Posidonienschiefers" in Western Switzerland (Etter, 2014a). These sequences record the Toarcian OAE, also known as the Posidonienschifer Event. Ammonoids were found in association with the bivalves *Bositra* sp. (="*Posidonia*" sp.), *Pseudomytiloides dubius* Sowerby, *Unicardium* sp., and *Solemya voltzi* Roemer.

Data from SEM and X-ray analyses (Fig. 4; Table S1) indicate that our cephalopod and bivalve mollusc shells, collected in this locality, are suitable for isotopic investigation.

Sr isotope results were obtained from two samples, taken from several ammonoid shells collected at this locality: (1) sample HS1 (material from eight cream-colored *Hildaites serpentinum* shells, 20–50 mm in diameter; about 74.0% aragonite with traces of α-SiO_2); and (2) sample HF1 (material from 10 cream-colored *Harpoceras falciferum* shells, 20–40 mm in diameter, about 79.0% aragonite with traces of α-SiO_2). The Sr isotope ratios, obtained from samples HS1 and HF1 are comparatively low: 0.707300 and 0.707382, respectively (Table S1). Other isotope data obtained from lower Toarcian cephalopod and bivalve molluscs of this locality are given in Table 1, revealing, in particular, comparatively high palaeotemperature of their living environment (25.2–32.0 °C).

Ryazan area (*lower upper Callovian*). Sr isotope data have been obtained from a Callovian *Procerites funatus* Oppel, specimen 55-1 from the Elatma River (Fig. 3). It is a mid-sized (38 mm in diameter), silvery-white shell. The Sr-isotope ratio in material taken at H = 10 mm is comparatively low ($^{87}Sr/^{86}Sr = 0.707429$; Table S1). $\delta^{18}O$ and $\delta^{13}C$ values have been obtained earlier from lower upper Callovian *Cosmoceras aculatum* Michailov (silvery-white shell, 100% aragonite), also from the Ryazan area. They are −1.3 and 3.3‰, respectively (Zakharov et al., 2006d), and indicate a palaeotemperature of 21.0 °C.

3.2.3. Holocene

We have analyzed the Sr isotope ratio in living *Nautilus pompilius* Linne from a shell that was collected in the Philippines (Bohol Island area). The investigated *Nautilus* shell, 101.2 mm in diameter, containing 27 septa, was caught at depth of about 180–250 m. The Sr isotope data was obtained from sample (S-23) taken from septum 23 at H = 270 mm ($^{87}Sr/^{86}Sr = 0.709148$; Fig. 3; Table S1).

Our previous $\delta^{18}O$ data (Zakharov et al., 2006a) suggests short-term vertical migration of this individual with an amplitude of several tens of meters. Just after hatching it likely lived in shallow water, following by a gradual migration to cooler, deeper waters. Thus, when it was a juvenile form with nine septa in its shell, it sank to a depth of about 200 m with temperature of water warmer than 16.8 °C. After building the 10th and 11th septa, it continued to sink, ultimately to a depth of about 300 m during formation of the 26th septum (water temperature of 13.7 °C). Septum 23 was secreted at temperature about 14 °C ($\delta^{18}O = 1.6‰$; $\delta^{13}C = 0.6‰$).

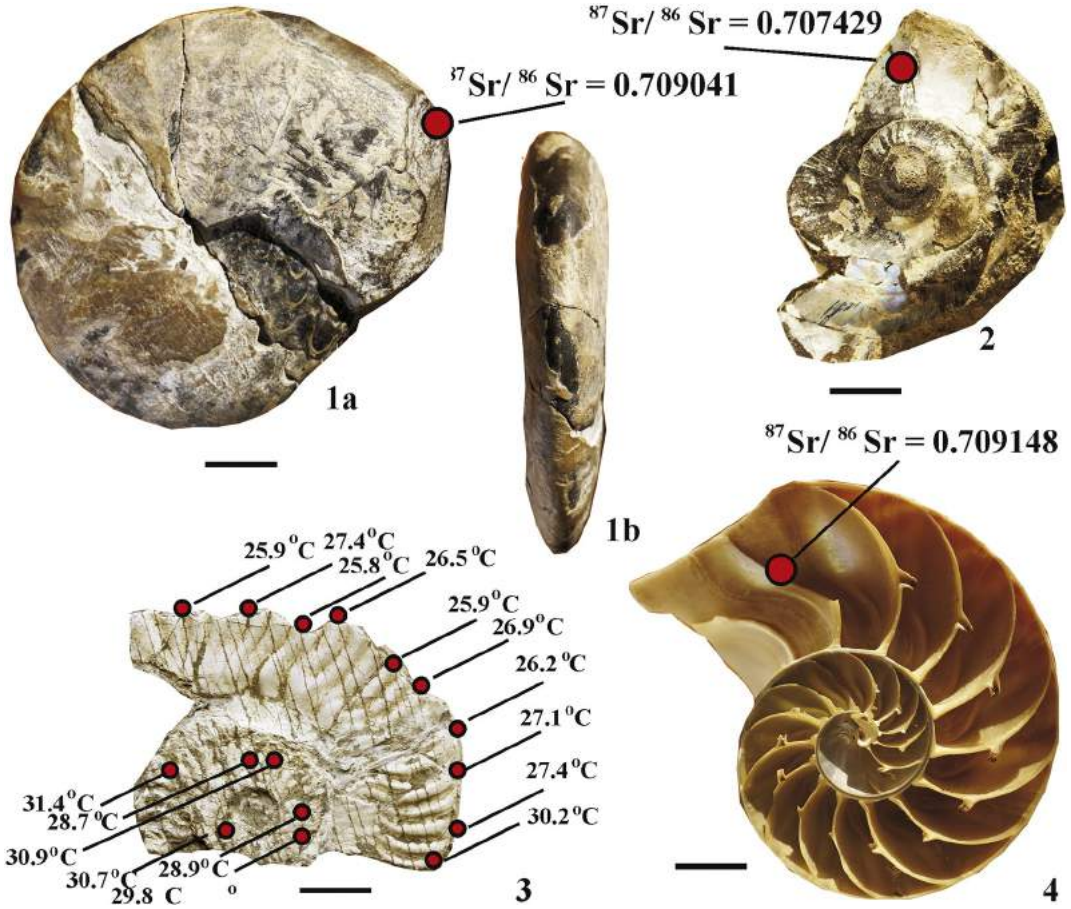

Fig. 3. Some investigated cephalopod shells: 1, *Boreomeekoceras keyserlingi* (Mojsisovics), Mengilyakh Creek, 45/802, Olenek River, uppermost Olenekian, Spiniplicatus Zone; 2, *Procerites funatus* Oppel, 55/1, Russian Platform, Ryazan area, Elatma River, upper Callovian; 3, *Hildaites serpentinum* Buckman, HS/2, Teysachaux mountain, Western Switzerland; lower Toarcian, "Posidonia Shale"; 4, living *Nautilus pompilius* Linne, Bohol Island area, Philippines. Scale bars = 10 mm.

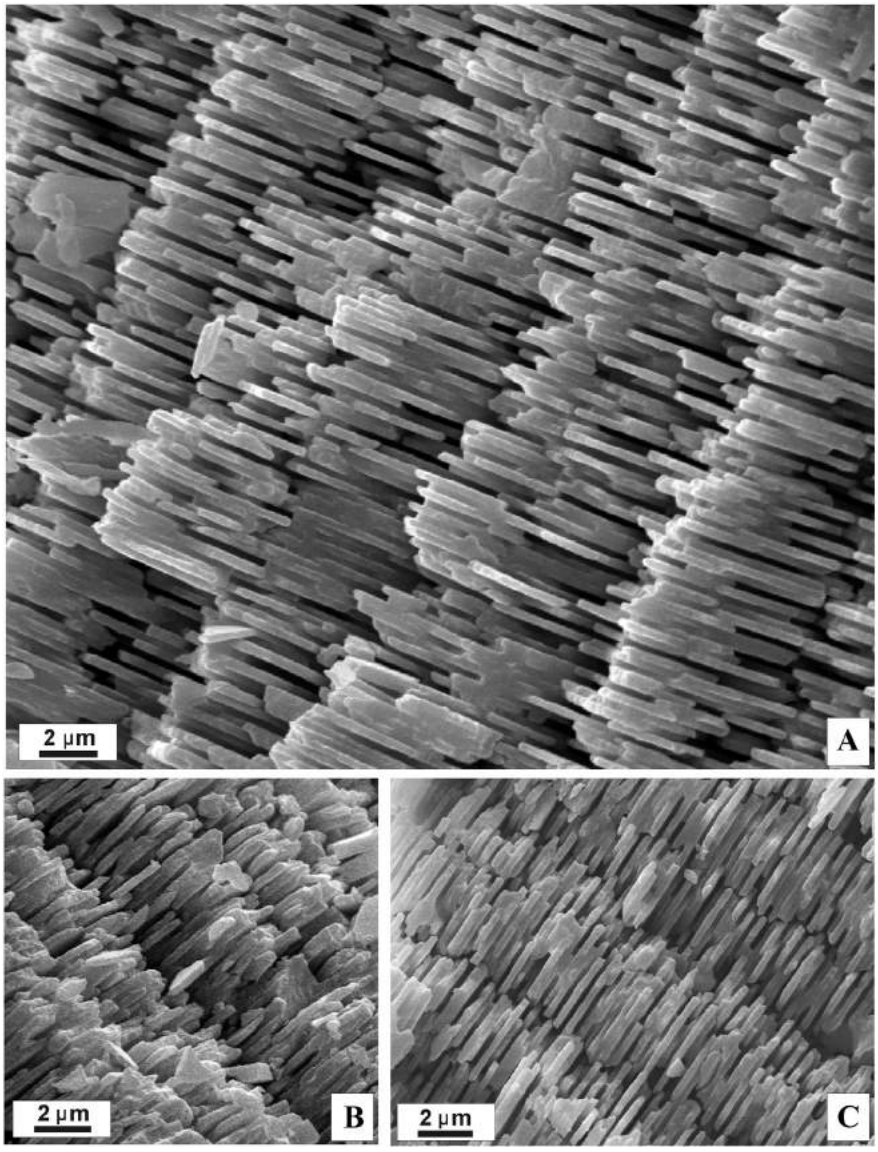

Fig. 4. SEM photomicrographs of lower Toarcian ammonoid shells: A, Phyllocreatidae? gen. et sp. indet., HS/29; B, *Harpoceras falciferum* Sowerby, HS/9; C, *Hildaites serpentinum* Buckman, HS/2; Teysachaux mountain, Western Switzerland, lower Toarcian, "Posidonia Shale".

4. Discussion

4.1. N isotope cycles

According to Algeo et al. (2014), the Phanerozoic $\delta^{15}N_{sed}$ curve has a strong relationship with first-order climate cycles, with low values occurring during the greenhouse climate modes of the Cretaceous, as well as mid-Jurassic and mid-Permian and high values occurring during the icehouse climate modes of the mid-Palaeozoic and Cenozoic. Cretaceous strata are greatly ^{15}N-depleted (−4 to 0‰), whereas Carboniferous units are highly ^{15}N-enriched (+6 to +14‰). Induan and lowest Olenekian units in South Primorye (Abrek Bay) are characterised mostly by positive $\delta^{15}N$ values, but higher in the lower part of the Olenekian the $\delta^{15}N$ values are negative (Zakharov et al., in press), possibly indirectly illustrating a local warming trend during the early Olenekian.

4.2. Climate (O isotope) cycles

On the basis of published and original data on O isotope composition of some Mesozoic fossils, mentioned above, 8 first-order climate cycles, represented by temperature maxima and minima, can be recognized in the Mesozoic (Fig. 5).

First-order Mesozoic temperature maxima occurred in the following: (1a) late early Olenekian (latest Smithian); (2a) late Sinemurian; (3a) early Toarcian; (4a) Bathonian; (5a) mid Tithonian; (6a) early Aptian; (7a) late Cenomanian-early Turonian; (8a) late Santonian-early Campanian.

They were accompanied apparently by the following first-order climatic minima: (1b) late Norian; (2b) late Pliensbachian; (3b) late Bajocian; (4b) Callovian; (5b) latest Barremian; (6b) late Aptian; (8b) Maastrichtian (Fig. 5).

4.3. C isotope cycles, Oceanic Anoxic Events (OAEs), and oceanic red-bed facies

Mesozoic OAEs have been documented in both Cretaceous (lower Aptian OAE 1a, lowermost Albian OAE 1b, lower upper Albian OAE 1c, latest Albian OAE 1d, uppermost Cenomanian OAE 2, and local Coniacian-Santonian OAE 3) (e.g., Erbacher, 1994; Wilson and Noris, 2001; Wagreich, 2009, 2012; Aquit et al., 2016) and the Jurassic (Toarcian OAE; Jones and Jenkyns, 2001). Among these, OAE 1a

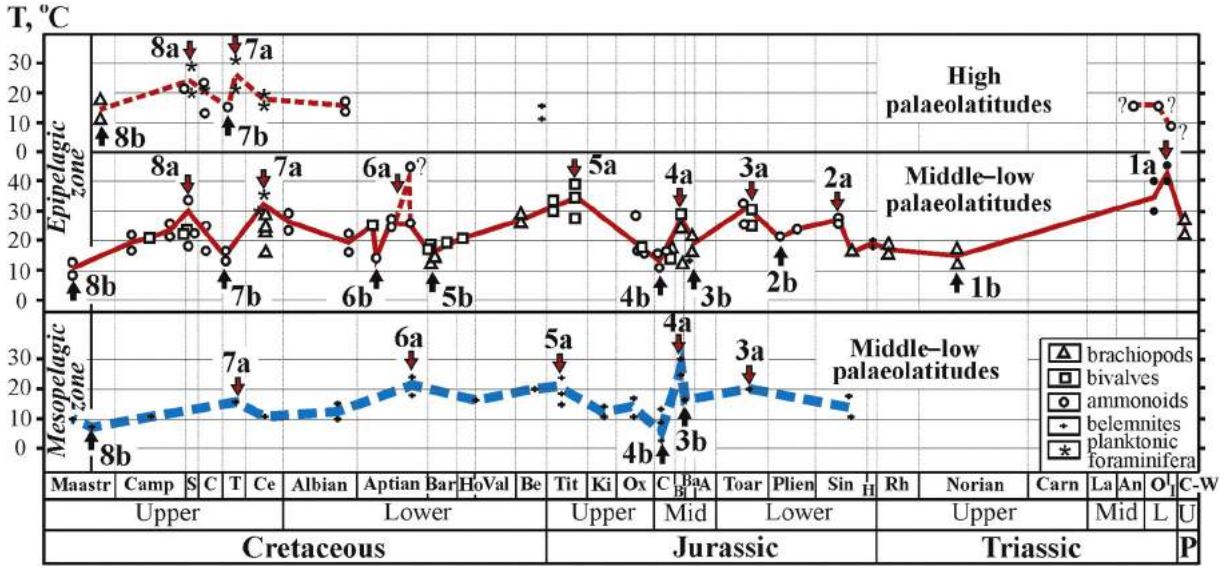

Fig. 5. A summary diagram showing variation of isotopic palaeotemperatures during the Late Permian–Late Cretaceous. The difference in the palaeotemperatures calculated from oxygen-isotopic composition of belemnite rostra and skeletons of most other fossils likely indicate that they were secreted in different depth conditions (mesopelagic and epipelagic zones, respectively). Temperature maxima: Olenekian (1a), late Sinemurian (2a), early Toarcian (3a), Bathonian (4a), middle Tithonian (5a), early Aptian (6a), late Cenomanian-early Turonian (7a), late Santonian-early Campanian (8a). Temperature minima: late Norian (1b), late Pliensbachian (2b), late Bajocian (3b), Callovian (4b), latest Barremian (5b), late Aptian (6b), late Turonian (7b), Maastrichtian (8b). Abbreviated stage, series and period names are: C-W, Changhsingian–Wuchiapingian; I, Induan, O, Olenekian; An, Anisian, La, Ladinian; Carn, Carnian; Rh, Rhaetian; H, Hettangian; Sin. Sinemurian; Plien, Pliensbachian; Toar, Toarcian; A, Aalenian; Ba, Bajocian; B, Bathonian; C, Callovian; Ox, Oxfordian; Ki, Kimmeridgian; Tit, Tithonian; Be, Berriasian; Val, Valanginian; Ho, Houterivian; Bar, Barremian; Ce, Cenomanian; T, Turonian; C, Coniacian; S, Santonian; Camp, Campanian; Maastr, Maastrichtian; L – Lower, Mid, Middle; U, Upper; P, Permian. References: Fritz, 1965; Teiss et al., 1968; Bowen, 1969; Fabricius et al., 1970; Kaltenegger et al., 1971; Teiss and Naidin, 1973; Anderson et al., 1994; Price and Sellwood, 1994; Ditchfield et al., 1994; Huber et al., 1995, 2002; Ditchfield, 1997; Norris and Wilson, 1998; Podlaha et al., 1998; Zakharov et al., 1999a, 1999b, Zakharov et al., 2001, Zakharov et al., 2006b, 2006c, 2006d, Zakharov et al., 2009, Zakharov et al., 2011, Zakharov et al., 2016, Zakharov et al., 2017a, 2017b; Price et al., 2000; Malchus and Steuber, 2002; Gröcke et al., 2003; Voigt et al., 2003; McArthur et al., 2004; Price and Mutterlose, 2004; V.A. Zakharov et al., 2005; Lécuyer and Bucher, 2006; Wierzbowski and Joachimski, 2007; Price and Rogov, 2009; Goudemand et al., 2013; Price and Passey, 2013; Rosales et al., 2004; Wierzbowski and Rogov, 2011; Joachimski et al., 2012; Sun et al., 2012; Romano et al., 2013; Wierzbowski et al., 2013; Schobben et al., 2014; Grigoryan et al., 2015; Dzyuba et al., 2013, 2017. Palaeotemperature data from Triassic conodonts are shown by black circles.

(Weissert-event) has received the most research effort. The bituminous shale member that records OAE 1a in the Ulianovsk area (up to 10.5 m thick) is located mostly in the upper part of the lower Aptian Volgensis–Schilovkensis Zone and was formed during a eustatic transgression (Gavrilov et al., 2002) under a warm climate (Zakharov et al., 2013a). Its lower part is characterised by the negative C isotope excursion; the positive C isotope excursion has been recognized somewhat higher up in the stratigraphy, in the lower Aptian Deshayesi–Tuberculatum Zone (Zakharov et al., 2013a). No benthic taxa were discovered in the Volgensis–Schilovkensis Zone of the Ulyanovsk area.

Taking into account that the Turonian–Campanian interval was the main depositional phase of the Cretaceous oceanic red beds (Wang et al., 2005, 2009; Wagreich, 2009, 2012; Hu et al., 2012), it can be concluded that the main period of development of the OAEs in the Mesozoic (Toarcian–Cenomanian) was followed by the period characterised by oxygen-rich deep waters in most of the oceans (Turonian–Campanian red-bed facies [Wang et al., 2005] and upper Campanian methane-seep facies [Cochran et al., 2016]).

Based on the C isotope composition of living *Nautilus* and brachiopods obtained from the Philippines (Zakharov et al., 2006a) and information on solar activity during the years 1991–1999 (solar cycles 22 and 23; Gnezdilov, 2004), when the investigated shells were secreted, we suspect, following Alcala-Herrera et al. (1992), that $\delta^{13}C$ fluctuations are mostly connected with fluctuations of phytoplankton bioproductivity, partly related to oscillations between low and high solar activity (sunspot cycles).

About 30 positive $\delta^{13}C$ excursions have been recognized from different stages of the Phanerozoic (Zakharov et al., 2006c, Fig. 62), ten of them are known in the Cretaceous. The majority of them coincided with episodes of volcanic activity that are proposed as to have been one of main sources of excess CO_2 (e.g., Weissert and Erba, 2004; Naafs et al., 2016). The most prominent negative C isotope excursion occurs globally in the Permian–Triassic boundary beds (e.g., Baud et al., 1989; Holser et al., 1991).

4.4. Sr isotope cycles

The published Sr-calibration curves for the Phanerozoic are based mostly on analyses of calcite and apatite fossil material and samples of whole rock. Our results from aragonite-preserved fossil material with good diagenetic control are useful for both corroboration of published Sr data and also for the minor correction of data points in some little-studied intervals.

The $^{87}Sr/^{86}Sr$ ratios of recent oceans are considered to be mainly a mixture of continental and hydrothermal (oceanic) flux (0.7120 and 0.7035, respectively; Davis et al., 2003). Riverine mass flux (continental flux) is almost certainly higher today than at any time during the Phanerozoic (Edmond, 1992).

4.4.1. Jurassic-Cretaceous

It has been suggested that the most prominent ophiolite pulses in the Mesozoic occurred during the Jurassic-Cretaceous (Toarcian–Berriasian and Aptian–Campanian; e.g., Dilek, 2003). We agree with some authors (Jenkyns et al., 1995; Jones and Jenkyns, 2001) that the prominent negative Sr isotope excursions known from the Mesozoic (e.g., Aptian-Albian and Late Cretaceous) were the result of strong plate tectonic activity. It might be partly connected with the opening of the Atlantic Ocean, which was followed by enhanced hydrothermal activity at the mid-ocean ridges (mantle volcanism) that supplied low radiogenic Sr to seawater. Most of these events were accompanied by significant sea-level changes, warming and Oceanic Anoxic Events (OAEs) that coincided closely in time. Comparatively low $^{87}Sr/^{86}Sr$ ratios were calculated by us from aragonitic ammonoid shells from the mid lower Aptian (0.707333–0.707382), lower Albian (0.707242–0.707276), upper

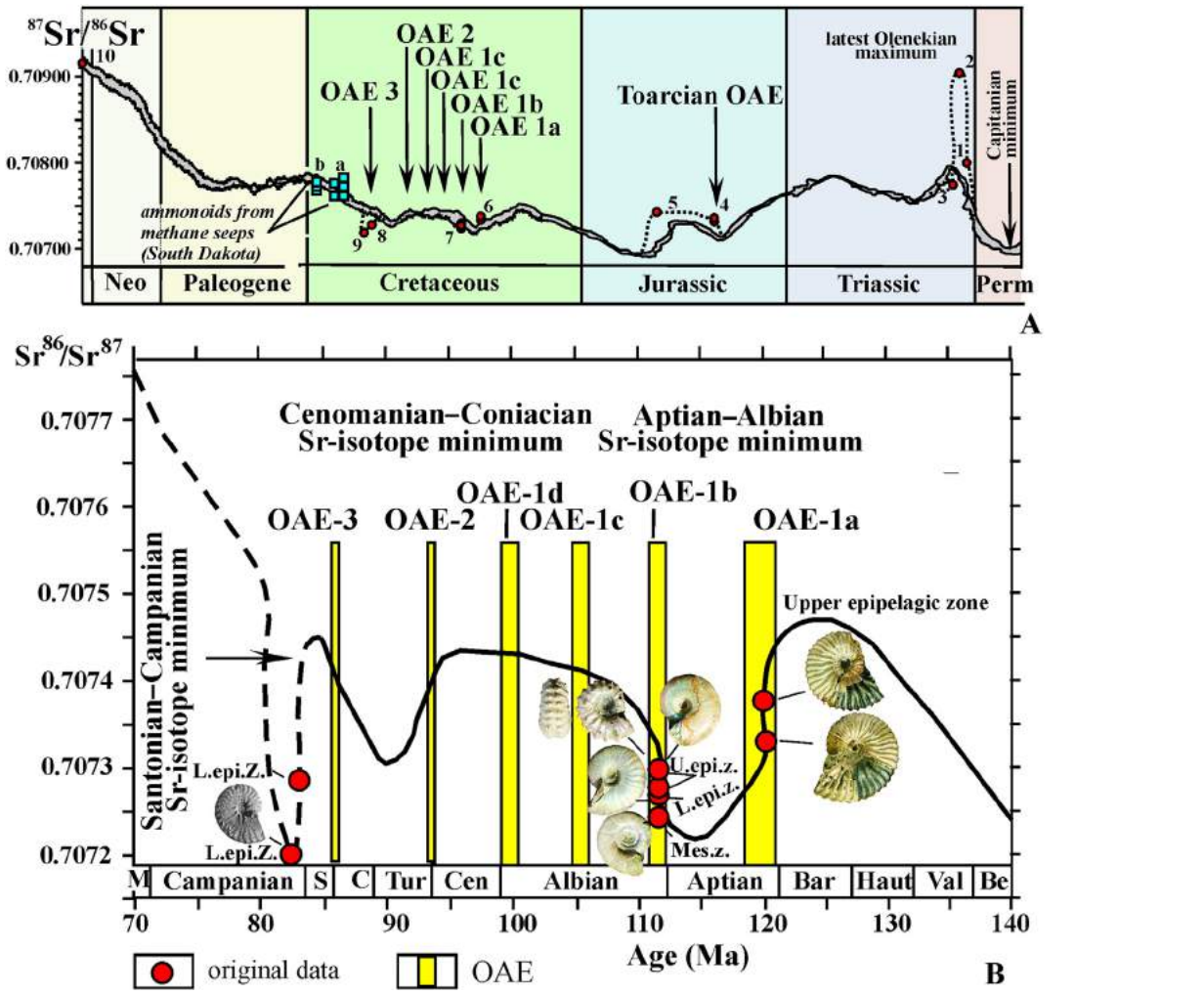

Fig. 6. Seawater Sr isotope curves: A, variant of McArthur et al. (2012), corrected; B, variant of Jones and Jenkyns (2001), corrected. Abbreviations: Perm, Permian; Neo, Neogene; Be, Berriasian; Val, Valanginian; Haut, Hauterivian; Bar, Barremian; Cen, Cenomanian; Tur, Turonian; C, Coniacian; S, Santonian; M, Maastrichtian; L.*epi.z*, Lower epipelagic zone; Mes.z, Mesopelagic zone; U.epi.z, Upper epipelagic zone.

Santonian (0.707333), and lower Campanian (0.707198) (Fig. 6), as well as from lower Toarcian (0.707300–0.707382) and lower upper Callovian (0.707429).

At the same time, the relatively higher and more variable $^{87}Sr/^{86}Sr$ ratios for some of the aforementioned intervals have been recently reported from deposits of some local areas, for instance in limestones of the upper Aptian–lower Albian Mural Formation in Mexico (0.707479–0.708790); the latter suggest significant weathering of local granitic provenance (Madhavaraju et al., 2015).

A final consideration that must be taken into account in our study is the problem of the strontium isotope stratification of the water column of Phanerozoic marine basins. Some efforts to understand this problem have been made in a study of the Albian of Madagascar (Zakharov et al., 2016). A gradual decrease of Sr-isotope ratio from 0.707296 to 0.707241 has been discovered in the following ammonoid shells, secreted in habitats from shallow to deeper zones of the water column: *Desmoceras* (0.707296), an inhabitant of the upper epipelagic zone; *Douvilleiceras* (0.707276), an inhabitant of the same zone; *Cleoniceras* (0.707275), an inhabitant of the deeper (likely lower epipelagic zone); and *Eogaudryceras* (0.707241), an inhabitant of the deeper, likely upper mesopelagic zone.

4.4.2. Other intervals investigated

The Paleozoic seawater Sr isotope curve reached its lowest equilibrium $^{87}Sr/^{86}Sr$ ratio in the Capitanian before rebounding to more strongly radiogenic values during the Permian/Triassic transition (Korte et al., 2006; McArthur et al., 2012; Kani et al., 2013; Kani et al., in press). The Capitanian low point may have its origins in the unusually strong ophiolite activity, taking into account (1) the Middle Permian Emeishan activity in South China, generated apparently by the opening of the Neotethys Ocean along the eastern margin of Gondwana during the Permian (e.g., Korte et al., 2006); (2) emplacement of contemporaneous Uralian ophiolites prior to the collision of Baltica-Eastern Europe and Kazakhstan-Siberia and closure of the Pleionic Ocean during the Late Permian (e.g., Dilek, 2003) and Siberian Trap activity of Late Permian age (e.g., Sadovnikov, 2016). As a result, a highly enhanced flux of low radiogenic Sr to seawater took place during Mid-Late Permian. In an alternative hypothesis, the Capitanian minimum was mainly caused by a decrease in the continental weathering rate due to the Mid Permian cooling that may have driven extensive ice-cover over continental crust to suppress continental flux enriched in high radiogenic Sr into the Ocean (Kani et al., 2013). Here we concur with the former model, because the latter is in disagreement with evidence for a dramatic Cenozoic rise in seawater $^{87}Sr/^{86}Sr$ that corresponded to times of progressive cooling and glaciation (François et al., 1993; Jones and Jenkyns, 2001).

On the contrary, the Lower Triassic is characterised by the maximum upward (more radiogenic) shift in the Sr isotope curve for the entire Mesozoic (an increase of $^{87}Sr/^{86}Sr$ ratio from 0.708043 to 0.709041 has been discovered in the Olenekian interval; Fig. 6). This is apparently due to significant expansion of dry land surfaces, partly because of the Dabie-Sulu Triassic orogeny in central-eastern China, created by

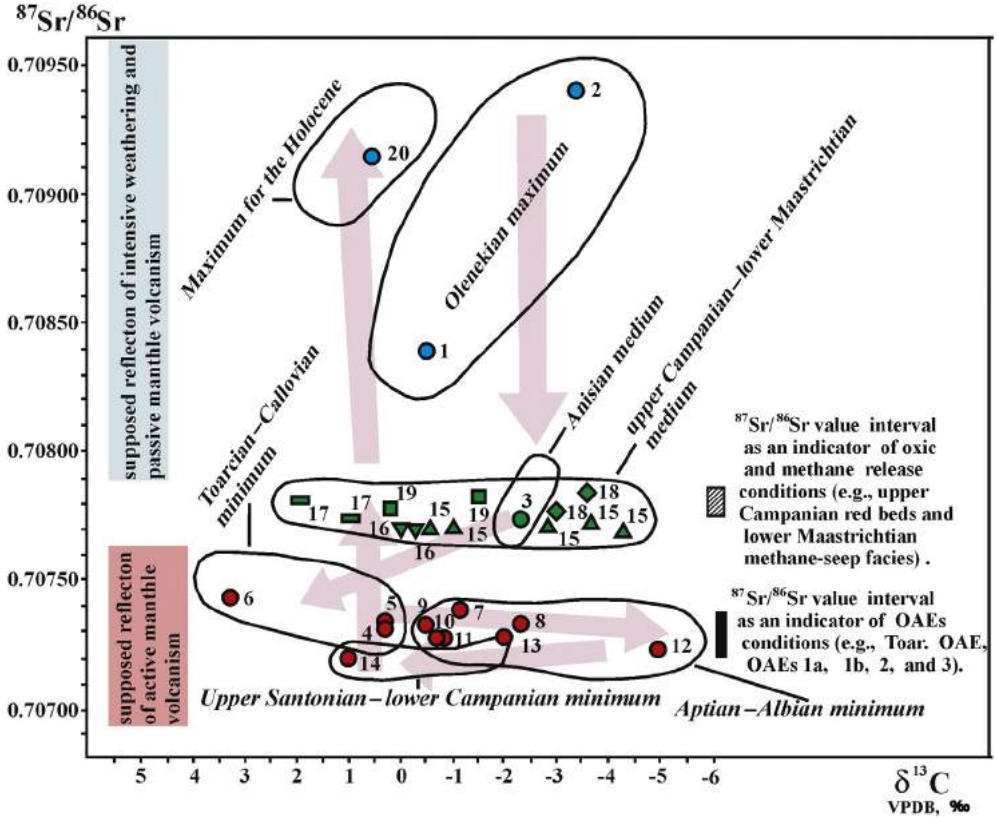

Fig. 7. Fluctuations in cephalopod environments during the Mesozoic and Cenozoic (Holocene): evidence from Sr and C isotope data. 1, lowermost Olenekian *Hedenstroemia*; 2, uppermost Olenekian *Boreomeekoceras*; 3, mid Anisian *Arctohungarites*; 4 and 5, lower Toarcian ammonoids; 6, upper Callovian *Procerites*; 7–12, lower Aptian–lower Albian ammonoids; 13, upper Santonian *Pseudoschloenbachia;* 14, lower Campanian *Submortoniceras*; 15–19, upper Campanian–lower Maastrichtian ammonoids (five species; Cochran et al., 2003, 2016); 20, living *Nautilus*. Time sequence is indicated by the arrows.

northward subduction of the Yangtze cratonal plate beneath the Sino-Korean craton (Zhang et al., 2009; Hacker et al., 2004; Isozaki et al., 2017) and their intensive weathering in conditions of extreme warming and aridity at the very end of the Smithian, which was followed by the development of warm and humid conditions in the late Spathian. The resulting excess weathering likely resulted in a global-scale input of a significant amount of high radiogenic Sr through riverine flux. Alternatively, the Olenekian maximum recorded in Arctic Siberian might be partly caused by brackish environments (the Sr isotope composition of fossils is used by Wierzbowski (2013; Wierzbowski et al., 2013) as an indicator of palaeosalinity, which needs confirmation).

The comparatively high $^{87}Sr/^{86}Sr$ ratio (0.709148), obtained by us from the living *Nautilus pompilius* shell is probably connected mainly with both the Alpine orogeny, accompanied by significant continental weathering and coming of high radiogenic Sr to seawater, and the weakening of mantle volcanism (Fig. 7).

5. Conclusions

Following (in part) Jones and Jenkyns (2001), we assume that there is a close temporal correspondence between episodes of increased hydrothermal activity at mid-ocean ridges, negative seawater Sr-isotope excursions, climatic warming and sea level rises, that usually resulted in the Aptian–Campanian OAEs. According to our data (Figs 5, 6), the Aptian and Santonian–Campanian Sr-isotope minima seem to be corresponded to climatic warming (marked as 6a and 8a, respectively), but Turonian–Coniacian and late Maastrichtian Sr-isotope maxima, in contrast, to climatic cooling (7b and 8b, respectively), However, there is no any clear correspondence in general between $\delta^{18}O$ and Sr-isotope records, especially for Late Permian–Jurassic and. Cenozoic times. The most distinctive feature of the Phanerozoic Sr isotope record is an exceedingly large swing in $^{87}Sr/^{86}Sr$ ratio between the Capitanian minimum (0.706800–707,000 in South Primorye; Kani et al., in press) and the Olenekian maximum (0.708043–0.709041). This seems to be mostly a result of enhanced Early–Mid Permian ophiolite activity and, on the other hand, the significant expansion of dry land surfaces (partly because of Dabie-Sulu orogeny) and their intensive weathering in conditions of extreme warming during much of the Early Triassic. These conditions gave way to warm and humid conditions in the latest Olenekian, which apparently released a significant amount of high radiogenic Sr via the riverine flux.

There are some hypotheses of cyclic or pulsating development of Earth conditions under impact of cosmic factors (e.g., Yepifanov, 2012a, 2012b; Barash, 2015). Data at least on early and late Mesozoic O and N isotope cycles seem to be in agreement with this idea, taking into account, for instance, information on long period cycles in the Earth's climate (galactic seasons). However, suitable information on Sr isotope cycles of the Earth is too limited in this stage of our knowledge to discuss on this topic, although periodicity in some processes, responsible for some fluctuations in seawater $^{87}Sr/^{86}Sr$ (e.g., mantle plume activities and orogenic events) inclines us to take interest in it.

Supplementary data to this article can be found online at https://doi.org/10.1016/j.sedgeo.2017.11.011.

Acknowledgments

We thank Dr. T.A. Velivetskaya and Mrs. V.M. Avchenko (DVGI, Vladivostok) for O and C isotope measurements, three anonymous reviewers, Prof. B. Jones (Editor, Sedimentary Geology) and Prof. K. Tanabe (The University Museum and the Department of Earth and Planetary Science, The University of Tokyo) for providing valuable editorial comments that substantially improved our paper, Prof. V.I.

Myslovets (Moscow State Univ.), Dr. V.A. Yepifanov (SNIIGIMS, Novosibirsk) and Dr. I.V. Kemkin (DVGI, Vladivostok) for help with acquisition of literature data, Dr. J.W. Haggart (Geol. Survey of Canada), Mr. G. Beard (Qualicum Beach Museum, Vancouver), and Dr. D.G. Lazo (The Univ. of Buenos Aires) for organization of the field excursions to Vancouver and Patagonia, Dr. E.S. Sobolev (Inst. of Petroleum Geol. and Geoph., Novosibirsk) and Dr. O.P. Smyshlyaeva (DVGI, Vladivostok) for their help in collecting mollusc shells from Toarcian shales in Western Switzerland. Our cordial thanks are due to Dr. David Bond (The Univ. of Hull, UK) for assistance with the manuscript. This work was partly supported by the Russian Foundation for basic Research, grant 18-05-00023.

References

Alcala-Herrera, J.A., Grossman, L.L., Gartner, S., 1992. Nannofossil diversity and equitability and fine-fraction $\delta^{13}C$ across the Cretaceous/Tertiary at Walvis Ridge Leg 74, South Atlantic. Marine Micropaleontology 20, 77–88.

Algeo, T.J., Meyers, P.A., Robinson, R.S., et al., 2014. Icehouse-greenhouse variations in marine denitrification. Biogeosciences 11, 1273–1295.

Anderson, T., Popp, B.N., Williams, A.C., Ho, L.Z., Hudson, J.D., 1994. The stable isotopic records of fossils from the Peterborough Member, Oxford Clay Formation (Jurassic), U.K.: paleoenvironmental implications. Journal of the Geological Society of London 151 (1), 125–138.

Aquit, M., Kuhnt, W., Holbourn, A., et al., 2016. Complete archive of late Turonian to early Campanian sedimentary deposition in newly drilled cores from the Tarfaya Basin, SW Morocco. Geological Society of America Bulletin https://doi.org/10.1130/B31523.1.

Banner, J.L., 2004. Radiogenic isotopes: systematics and applications to earth surface processes and chemical stratigraphy. Earth-Science Reviews 65, 141–194.

Barash, M.C., 2015. Prichiny Katastroficheskikh Massovykh Vymiranij v Fanerozoye (Reasons of the Catastrophic Mass-Extinctions in the Phanerozoic). Lambert Academic Publishing, Saarbrücken (143 pp. (in Russian)).

Baud, A.M., Magaritz, M., Holser, W.T., 1989. Permian–Triassic of the Tethys: carbon isotope stratigraphy. Geologische Rundschau 78, 649–677.

Bowen, R., 1969. Palaeotemperature Analysis. Izdatel'stvo "Nedra", Leningrad (207 pp. (in Russian)).

Brass, G.W., 1976. The variation of the marine $^{87}Sr/^{86}Sr$ ratio during Phanerozoic time: interpretation using a flux model. Geochimica et Cosmochimica Acta 40, 721–730.

Burke, W.H., Denison, R.E., Hetherington, E.A., Koepnick, R.B., Nelson, H.F., Otto, J.B., 1982. Variation of seawater $^{87}Sr/^{86}Sr$ throughout Phanerozoic time. Geology 10, 516–519.

Clements, S.C., Farell, J.W., Grometn, L.P., 1993. Synchronous changes in seawater strontium isotope composition and global climate. Nature 363, 607–610.

Cochran, J.K., Landman, N.H., Turekian, K.K., Michard, A., Schrag, D.P., 2003. Paleoceanography of the Late Cretaceous (Maastrichtian) Western Interior Seaway of North America: evidence from Sr and O isotopes. Palaeogeography, Palaeoclimatology, Palaeoecology 191, 45–64.

Cochran, J.K., Landman, N.H., Larson, N.L., Meehan, C., Garb, M., Brezina, J., 2016. Swiss Journal of Palaeontology 134:153–165. https://doi.org/10.1007/s13358-015-0087-9 Online version at:.

Coplen, T.B., Kendall, C., Hopple, J., 1983. Comparison of stable isotope reference samples. Nature 302, 236–238.

Davis, A.C., Bickle, M.J., Teagle, D.A.H., 2003. Imbalance in the oceanic strontium budget. Earth and Planetary Science Letters 66, 191–213.

Degryse, P., Schneider, J., 2008. Pliny the elder and Sr–Nd isotopes: tracing the provenance of raw materials for Roman glass production. Journal of Archaeological Science 35, 1993–2000.

Denison, R.E., Koepnick, R.B., Burke, W.H., Hetherington, E.A., Fletcher, A., 1994. Construction of the Mississippian, Pennsylvanian and Permian seawater $^{87}Sr/^{86}Sr$ curve. Chemical Geology 112, 145–167.

Denison, R.E., Miller, N.R., Scott, R.W., Reaser, D.F., 2003. Strontium isotope stratigraphy of the Comanchean series in North Texas and southern Oklahoma. Geological Society of America Bulletin 115 (6), 669–682.

Dilek, Y., 2003. Ophiolite pulses, mantleplumes and orogeny. In: Dilek, Y., Robinson, P.T. (Eds.), Ophiolites in Earth History. The Geological Society of London, London (Special Publication) 218, pp. 9–19.

Ditchfield, P.W., 1997. High northern palaeolatitude Jurassic–Cretaceous palaeotemperature variations: new data from Kong Karls Land, Svalbard. Palaeogeography, Palaeoclimatology, Palaeoecology 130, 163–175.

Ditchfield, P.W., Marshall, J.D., Pirrie, D., 1994. High latitude palaeotemperature variation: new data from the Tithonian to Eocene of James Ross Island, Antarctica. Palaeogeography, Palaeoclimatology, Palaeoecology 107, 79–101.

Dzyuba, O.S., Izokh, O.P., Shurygin, B.N., 2013. Carbon isotope excursions in Boreal Jurassic-Cretaceous boundary section and their correlation potential. Palaeogeography, Palaeoclimatology, Palaeoecology 381–382, 33–46.

Dzyuba, O.S., Guzhikov, A.Y., Manikin, A.G., et al., 2017. Magneto- and carbon isotope stratigraphy of the lower–middle Bathonian of the Sokur Tract section (Saratov, Central Russia): implications for global correlation. Geologiya and Geophizika 58 (2), 250–272 (in Russia).

Edmond, J.M., 1992. Himalayan tectonics, weathering processes, and the strontium isotope record in marine limestones. Science 258, 1594–1597.

Erbacher, J., 1994. Entwicklung und Paläooxeanographie mittelkretazischer radiolarian der westlichen Tethys (Italien) und des Nordatlantiks. Tübinger Mikro-Paläontologische Mitteilungen 1994 (12), 1–120.

Etter, W., 2014a. Alpine "Posidonia Shale" (Lower Toarcian, "Couches du Creux de l'Ours") in the Prealps of western Switzerland. In: Klug, C., Etter, W. (Eds.), Field Guide to the Excursions. Fossillagerstätten of the Southern German Jurassic. Mesozoic Ammonoid Localities of Switzerland and Eastern France. 9th International Symposium "Cephalopods – Present and Past". Universitat Zürich, Zürich, pp. 29–32.

Etter, W., 2014b. Condensed uppermost Bathonian-lowermost Callovian at Anwil canton Baselland, northern Switzerland. In: Klug, Ch., Etter, W. (Eds.), Mesozoic Ammonoid Localites of Switzerland and Eastern France (Field Guide to Excursion, 9th International Symposium Cephalopod–Present and Past, 2014, Zürich, Austria). Palaontologisches Institut und Museum, Ubiversität Zürich, Zürich, pp. 43–50.

Fabricius, F., Friedrichsen, H., Jacobshagen, V., 1970. Paläotemperaturen und Paläoklima in Obertrias und Lias der Alpen. Geologische Rundschau 59 (2), 805–826.

François, L.M., Walker, J.C.G., Opdyke, B.N., 1993. The history of global weathering and chemical evolution of the ocean-atmosphere system. In: Takahashi, E., Jeanloz, R., Rabie, D.C. (Eds.), Evolution of the Earth and Planets. Geophysical Monograph 74. American Geophysical Union-International Union of Geodesy and Geophysics, Washington, D.C., pp. 143–159.

Fritz, P., 1965. O^{18}/O^{16}-Isotopenanalysen und Paleotemperatur bestimmungen an Belemniten aus dem schwäb. Jura. Geologische Rundschau 54, 261–269.

Gavrilov, Y.O., Shchepetova, E.V., Baraboshkin, E.Y., Shcherbinina, E.A., 2002. The Early Cretaceous Anoxic Basin of the Russian Plate: sedimentology and geochemistry. Lithology and Mineral Resources 37 (4), 310–329.

Gnezdilov, A.A., 2004. Shumovyye buri i evolutsiya koronalnykh struktur v 20–23 tsyklakh solnechnoj aktivnosti po dannym IZMIRAN Sound Storms and Evolution of Coronal Structure in 20–23 cycles of the Solar Activity from IZMIRAN Data. Site of the Laboratory of Sun Radiation. http://helios.izmiran.rssi.ru/ars/agnezdil/paper8.htm (in Russian).

Goudemand, N., Romano, C., Brayard, A., Hochuli, P.A., Bucher, H., 2013. Comment on "lethally hot temperatures during the Early Triassic greenhouse". Science 339 (1033a–1033c).

Grigoryan, A.G., Alekseev, A.S., Joachimski, M.M., Gatovsky, Y.A., 2015. Permian-Triassic biotic crisis: a multidisciplinary study of Armenian sections. XVIII International Congress on the Carboniferous and Permian, Kazan, Russia, August 11–15, 2015. Abstract Volume. Kazan Federal University, Kazan, p. 74.

Gröcke, D.R., Price, G.D., Ruffell, A.H., Mutterlose, J., Baraboshkin, E., 2003. Isotopic evidence for Late Jurassic–Early Cretaceous climate change. Palaeogeography, Palaeoclimatology, Palaeoecology 202, 97–118.

Grossman, E.L., Ku, T.-L., 1986. Oxygen and carbon isotope fractionation in biogenic aragonite: temperature effect. Chemical Geology 59, 59–74.

Hacker, B.R., Ratschbacher, L., Liou, J.G., 2004. Subduction, collision and exhumation in the ultrahigh-pressure Qinling-Dable orogen. In: Malpas, J., Pletcher, C.J.N., Ali, J.R., Aitchison, J.C. (Eds.), Aspects of the Evolution of China. Geological Society, London, Special Publications 226, pp. 157–175.

Hallam, A., 1969. Faunal realms and facies in the Jurassic. Palaeontology 12 (1), 1–18.

Hess, J., Bender, M.L., Schilling, J.-G., 1986. Evolution of the ratio of strontium-87 to strontium-87 to strontium-86 in seawater from Cretaceous to present. Science 231, 979–984.

Holser, W.T., Schönlaub, H.P., Borckelmann, K., Magaritz, M., 1991. The Permian–Triassic of the Gartnerkofel-1 core (Carnic Alps): synthesis and conclusions. Abhandlungen der Geologischen Bundesanstalt 45, 213–232.

Hostettler, B., 2014. The Argovian Middle and Late Jurassic in the quarry Jakobsberg (Jura Cement) at Auenstein and Holderbank. In: Klug, Ch., Etter, W. (Eds.), Mesozoic Ammonoid Localites of Switzerland and Eastern France (Field Guide to Excursion, 9th International Symposium Cephalopod–Present and Past, 2014, Zürich, Austria). Palaontologisches Institut und Museum, Universität Zürich, Zürich, pp. 36–42.

Hu, X., Scott, R.W., Cai, Y., Wang, C., Melinte-Dobrinescu, M.C., 2012. Cretaceous oceanic red beds (CORBs): different time scales and models of origin. Earth Science Reviews 115, 217–248.

Huber, B.T., Hodell, D.A., Amilton, Ch.P., 1995. Middle–Late Cretaceous climate of the southern high latitudes: stable isotopic evidence for minimal equator-to-pole thermal gradients. Geological Society of America Bulletin 107 (10), 1164–1191.

Huber, B.T., Norris, R.D., MacLeod, K.G., 2002. Deep-sea paleotemperature record of extreme warmth during the Cretaceous. Geology 30, 123–126.

Hudson, J.D., Anderson, T.F., 1989. Ocean temperatures and isotopic compositions through time. Transactions of the Royal Society of Edinburgh. Earth Science 80, 183–192.

Isozaki, Y., Nakahata, H., Zakharov, Y.D., Popov, A.M., Sakata, S., 2017. Greater South China extended to the Khanka block: detrital zircon geochronology of middle-upper Paleozoic sandstones in Primorye, Far East Russia. Journal of Asian Earth Sciences 145, 565–575.

Jenkyns, H.C., Paul, K., Cummins, D.I., Fullagar, P.D., 1995. Strontium-isotope stratigraphy of Lower Cretaceous atoll carbonates in the mid Pacific Mountains. Proceeding of the Ocean Drilling Program, Scientific Results 143, 89–97.

Jenkyns, H.C., Jones, C., Gröcke, D.R., Hesselbo, S.P., Parkinson, D.N., 2002. Chemostratigraphy of the Jurassic System: applications, limitations and implcations for palaeoceanography. Journal of the Geological Society 159, 351–378.

Joachimski, M.M., Lai, X., Shen, S., et al., 2012. Climate warming in the latest Permian and the Permian–Triassic mass extinction. Geology 40, 195–198.

Jones, C.E., Jenkyns, H.C., 2001. Seawater strontium isotopes, oceanic anoxic events, and seafloor hydrothermal activity in the Jurassic and Cretaceous. American Journal of Science 501, 112–149.

Jones, C.E., Jenkyns, H.C., Hesselbo, S.P., 1994. Strontium isotopes in Early Jurassic seawater. Geochimica et Cosmochimica Acta 58, 1285–1301.

Kaltenegger, W., Preisinger, A., Rögl, F., 1971. Palaeotemperature determinations of aragonitic mollusks from the Alpine Mesozoic. Palaeogeography, Palaeoclimatology, Palaeoecology 10, 273–285.

Kani, T., Hisanabe, C., Isozaki, Y., 2013. The Capitanian (Permian) minimum of $^{87}Sr/^{86}Sr$ ratio in the mid-Panthalassan paleo-atoll carbonates and its demise by the deglaciation and continental doming. Gondwana Research 24, 212–221.

Kani, T., Isozaki, Y., Hayashi, R., Zakharov, Y.D., Popov, A.M., 2017. $^{87}Sr/^{86}Sr$ minimum of the Phanerozoic detected in Capitanian (Middle Permian) shelf carbonates in NE Japan and Primorye (Far East Russia): reef collapse by global cooling? Palaeogeography, Palaeoclimatology, Palaeoecology (in press).

Koepnick, R.B., Denison, R.E., Burke, W.H., Hetherington, E.A., Dahl, D.A., 1990. Construction of the Triassic and Jurassic portion of the Phanerozoic curve of seawater $^{87}Sr/^{86}Sr$. Chemical Geology 80, 327–349.

Korte, C., Kozur, H.W., Bruckschen, P., Veizer, J., 2003. Strontium isotope evolution of Late Permian and Triassic seawater. Geochimica et Cosmochimica Acta 67, 47–62.

Korte, C., Kozur, H.W., Joachimski, M.M., Strauss, H., Veizer, J., Schwark, L., 2004. Carbon, sulfur, oxygen, and strontium isotope record, organic geochemistry and biostratigraphy across the Permian/Triassic boundary in Abadeh, Iran. International Journal of Earth Sciences (Geologische Rundschau) 93, 565–581.

Korte, C., Jasper, T., Kozur, H.W., Bruckschen, P., Veizer, J., 2006. $^{87}Sr/^{86}Sr$ record of Permian seawater. Palaeogeography, Palaeoclimatology, Palaeocology 240, 89–107.

Kürsteiner, P., 2014. The Cretaceous of the Alpstein. In: Klug, Ch., Etter, W. (Eds.), Mesozoic Ammonoid Localites of Switzerland and Eastern France (Field Guide to Excursion, 9th International Symposium Cephalopod–Present and Past, 2014, Zürich, Austria). Palaontologisches Institut und Museum, Universität Zürich, Zürich, pp. 43–50.

Lazo, D., Cataldo, C.S., Fernández, D.E., Luci, L., Vennari, V.V., 2014. A Cretaceous Marine Odyssey in the Neuqén Basin (Field Guide, 4th International Palaeontological Congress, September 28–October 3, 3014, Mendoza, Argentina), Neuqén, Conicet (50 pp.).

Lécuyer, C., Bucher, H., 2006. Stable isotope compositions of a late Jurassic ammonite shell: a record of seasonal surface water temperatures in the southern hemisphere? Earth 1, 1–7.

Lukeneder, A., Harzhauser, M., Müllegger, S., Piller, W.E., 2010. Ontogeny and habitat change in Mesozoic cephalopods revealed by stable isotopes ($\delta^{18}O$, $\delta^{13}C$). Earth and Planetary Science 296, 103–114.

Madhavaraju, J., Scott, R.W., Lee, Y.I., Bincy, K.S., González-León, C.M., Ramasamy, S., 2015. Facies, biostratigraphy, and depositional environments of Lower Cretaceous strata, Sierra San José section, Sonora (Mexico). Carnets de Géologie 15 (10), 103–122.

Malchus, N., Steuber, T., 2002. Stable isotope records (O, C) of Jurassic aragonitic shells from England and NW Poland: palaeoecologic and environmental implications. Geobios 35, 29–39.

Martin, E.E., MacDougell, J.D., 1995. Sr and Nd isotopes at the Permian/Triassic boundary: a record of climate change. Chemical Geology 125, 73–99.

McArthur, J.M., 1994. Recent trends in strontium isotope stratigraphy. Terra Nova 6, 331–358.

McArthur, J.M., Chen, M., Gale, A.S., Thirlwall, M.F., Kennedy, W.J., 1993. Strontium isotope stratigraphy for the Late Cretaceous: Age models and intercontinental correlations for the Campanian. Paleoceanography 8, 859–873.

McArthur, J.M., Donovan, D.T., Thirlwall, M.F., Fouke, B.W., Mattey, D., 2000. Strontium isotope profile of the Early Toarcian (Jurassic) Oceanic Anoxic Event, the duration of ammonite biozones, and belemnite palaeotemperatures. Earth and Planetary Science Letters 179, 269–285.

McArthur, J.M., Mutterlose, J., Price, G.D., Rawson, P.F., Ruffell, A., Thirlwall, M.F., 2004. Belemnites of Valanginian, Hauterivian and Barremian age: Sr-isotope stratigraphy, composition ($^{87}Sr/^{86}Sr$, $\delta^{13}C$, $\delta^{18}O$, Na, Sr, Mg) and palaeo-oceanography. Palaeogeography, Palaeoclimatology, Palaeoecology 202, 253–272.

McArthur, J.M., Howard, R.J., Shields, G.A., 2012. Strontium isotope stratigraphy. The Geological Time Scale https://doi.org/10.1016/B978-0-444-59425-9.00007-X (Online version at:).

McArthur, J.M., Steuber, T., Page, K.N., Landman, N.H., 2016. Sr-isotope stratigraphy: assigning time in the Campanian, Pliensbachian, Toarcian, and Valanginian. The Journal of Geology 124:569–586. https://doi.org/10.1086/687395 (Online version at:).

Mojsisovics, E., 1886. Arctische Triasfaunen. Beiträge zur paläontologischen Characteristik der arctisch-pazifischen Triasprovinz. Mémoires de l'Académie Imperiale des Sciences de St.-Pétersbourg (sér. 7) 33 (6), (159 pp.)

Naafs, B.D.A., Castro, J.V., De Gea, G.A., Quijano, M.L., Schmidt, D.N., Pancost, R.D., 2016. Gradual and sustained carbon dioxide release during Aptian Oceanic Anoxic Event 1a. Nature Geoscience https://doi.org/10.1038/NGEO2627.

Norris, R.D., Wilson, P.A., 1998. Low latitude sea-surface temperatures for the mid Cretaceous and the evolution of planktonic foraminifera. Geology 26, 823–826.

Pirrie, D., Marshall, J.D., 1990. High-paleolatitude Late Cretaceous paleotemperatures: new data from James Ross Island, Antarctica. Geology 18, 31–34.

Podlaha, O.G., Mutterlose, J., Veizer, J., 1998. Preservation of $\delta^{18}O$ and $\delta^{13}C$ in belemnite rostra from the Jurassic Early Cretaceous successions. American Journal of Science 298, 324–347.

Price, G.D., Hart, M.B., 2002. Isotopic evidence for Early to mid-Cretaceous ocean temperature variability. Marine Micropaleontology 46, 45–58.

Price, G.D., Mutterlose, J., 2004. Isotopic signals from late Jurassic–early Cretaceous ocean (Volgian-Valanginian) sub-Arctic belemnites, Yatria River, Western Siberia. Journal of the Geological Society of London 161, 959–968.

Price, G.D., Passey, B.H., 2013. Dinamic polar climates in a greenhouse world: evidence from clumped isotope thermometry of Early Cretaceous belemnites. Geology 41 (8), 923–926.

Price, G.D., Rogov, M.A., 2009. An isotopic appraisal of the Late Jurassic greenhouse phase in the Russian Platform. Palaeogeography, Palaeoclimatology, Palaeoecology 273 (1-2), 41–49.

Price, G.D., Sellwood, B.W., 1994. Palaeotemperatures indicated by Upper Jurassic (Kimmeridgian–Tithonian) fossils from Mallorca determined by oxygen isotopic composition. Palaeogeography, Palaeoclimatology, Palaeoecology 110, 1–10.

Price, G.D., Ruffell, A.H., Jones, C.E., et al., 2000. Isotopic evidence for temperature variation during the early Cretaceous (late Ryazanian–mid Hauterivian). Journal of the Geological Society of London 157, 335–343.

Prokoph, A., Shields, G.A., Veizer, J., 2008. Compilation and time-series analysis of a marine carbonate $\delta^{18}O$, $\delta^{13}C$, $^{87}Sr/^{86}Sr$ and $\delta^{34}S$ database through Earth history. Earth-Science Reviews 87, 113–133.

Romano, C., Goudemand, N., Vennemann, T.W., et al., 2013. Climatic and biotic upheavals following the end-Permian mass extinction. Nature Geoscience 6, 57–60.

Rosales, I., Robles, S., Quesada, S., 2004. Elemental and oxygen isotope composition of Early Jurassic belemnites: salinity vs. temperature signals. Journal of Sedimentary Research 74 (2), 342–354.

Sadovnikov, G.N., 2016. Evolution of the biome of the middle Siberian trappean plateau. Paleontological Journal 50 (5), 518–532.

Schobben, M., Joachimski, M.M., Korn, D., et al., 2014. Palaeotethys seawater temperature rise and an intensified hydrological cycle following the end-Permian mass extinction. Gondwana Research 26, 675–683.

Shackleton, N.J., Kennet, J.P., 1975. Paleotemperature history of the Cenozoic and the initiation of Antarctic glaciation. In: Kennett, J.P., Houtz, R.E., et al. (Eds.), Oxygen and Carbon Isotope Analyses in DSDP Sites 277, 279 and 281. Initial Reports of the Deep Sea Drilling Project 29. U.S. Government Printing Office, Washington, pp. 743–756.

Sun, Y., Joachimski, M.M., Wignall, P.B., et al., 2012. Lethally hot temperatures during the Early Triassic Greenhouse. Science 338, 366–370.

Teiss, R.V., Naidin, D.P., 1973. Palaeothermometry and Oxygen Isotopic Composition in Organogenic Carbonates. Izdatel'stvo "Nauka", Moscow (256 pp.(in Russian)).

Teiss, R.V., Naidin, D.P., Saks, V.N., 1968. Calculation of Late Jurassic and Early Cretaceous paleotemperatures from oxygen isotopic composition of belemnite rostra. Trudy Instituta Geologii i Geofiziki Akademii Nauk SSSR 48, 51–71 (in Russian).

Van Geldern, R., Joachimski, M.M., Day, J., Jansen, U., Alvarez, F., Yolkin, E.A., Ma, X.-P., 2006. Carbon, oxygen and strontium isotope records of Devonian brachiopod shell calcite. Palaeogeography, Palaeoclimatology, Palaeoecology 240, 47–67.

Veizer, J., Compston, W., 1974. $^{87}Sr/^{86}Sr$ composition of seawater during the Phanerozoic. Geochimica et Cosmochimica Acta 33, 1461–1484.

Veizer, J., Prokoph, A., 2015. Temperatures and oxygen isotopic composition of Phanerozoic oceans. Earth-Science Reviews 146, 92–104.

Veizer, J., Ala, D., Azmy, K., Bruckschen, P., Buhl, D., et al., 1999. $^{87}Sr/^{86}Sr$, $\delta^{13}C$ and $\delta^{18}O$ evolution of Phanerozoic seawater. Chemical Geology 161, 59–88.

Voigt, S., Wilmsen, M., Mortimore, R.N., Voigt, T., 2003. Cenomanian palaeotemperatures derived from the oxygen isotopic composition of brachiopods and belemnites: evaluation of Cretaceous palaeotemperature proxies. International Journal of Earth Sciences (Geologische Rundschau) 92, 285–299.

Wagreich, M., 2009. Coniacian–Santonian oceanic red beds and their link to Oceanic Anoxic Event 3. In: Hu, X., Wang, Ch., Scott, R.W., Wagreich, M., Jansa, L. (Eds.), Cretaceous Oceanic Red Beds; Stratigraphy, Composition, Origins, and Paleoceanographic and Paleoclimatic Significance. SEPM (Society for Sedimentary Geology), Special Publication 91, pp. 235–242.

Wagreich, M., 2012. "OAE 3" – regional Atlantic organic carbon burial during the Coniacian–Santonian. Climate of the Past 8, 1447–1455.

Wang, Ch., Hu, X., Sarti, M., Scott, R.W., Li, X., 2005. Upper Cretaceous oceanic red beds in southern Tibet: a major change from anoxic to oxic, deep-sea environments. Cretaceous Research 26, 21–32.

Wang, Ch., Hu, X., Huang, Y., Scott, R.W., Wagreich, M., 2009. Overview of Cretaceous oceanic red beds (CORBs): a window on global oceanic and climate change. In: Hu, X., Wang, Ch., Scott, R.W., Wagreich, M., Jansa, L. (Eds.), Cretaceous Oceanic Red Beds; Stratigraphy, Composition, Origins, and Paleoceanographic and Paleoclimatic Significance. SEPM (Society for Sedimentary Geology), Special Publication 91, pp. 13–33.

Ward, P.D., Haggart, J.W., Michell, R., Kirschvink, J.L., Tobin, T., 2012. Integration of macrofossil biostratigraphy and magnetostratigraphy for the Pacific coast Upper Cretaceous (Campanian–Maastrichtian) of North America and implications for correlation with the Western Interior and Tethys. Geological Society of America Bulletin 124 (5/6), 957–974.

Weissert, H., Erba, E., 2004. Volcanism, CO_2 and palaeoclimate: a Late Jurassic-Early Cretaceous carbon and oxygen isotope record. Journal of the Geological Society of London 161, 1–8.

Wierzbowski, H., 2013. Strontium isotope composition of sedimentary rocks and its application to chemostratigraphy and palaeoenvironmental reconstructions. Annales Universitatus Mariae Curie-Sklodowska 68, 23–37.

Wierzbowski, H., Joachimski, M., 2007. Reconstruction of late Bajocian–Bathonian marine palaeoenvironment using carbon and oxygen isotope ratios of calcareous fossils from the Polish Jura Chain (central Poland). Palaeogeography, Palaeoclimatology, Palaeoecology 254, 523–540.

Wierzbowski, H., Rogov, M.A., 2011. Reconstructing the palaeoenvironment of the Middle Russian Sea during the Middle–Late Jurassic transition using stable isotope ratios of cephalopod shells and variations in faunal assemblages. Palaeogeography, Palaeoclimatology, Palaeoecology 299, 250–264.

Wierzbowski, H., Rogov, M.A., Matyja, B.A., Kiselev, D., Ippolitov, 2013. Middle–Upper Jurassic (Upper Callovian–Lower Kimmeridgian) stable isotope and elemental records of the Russian Platform: Indices of oceanographic and climatic changes. Global and Planetary Change 107, 196–212.

Wilson, P.A., Noris, R.D., 2001. Warm tropical oceansurface and global anoxia during the mid-Cretaceous period. Nature 412, 425–429.

Wotte, T., Alvaro, J.-J., Shields, G.A., Brown, B., Brasier, M.D., Veizer, J., 2007. High resolution C-, O-, and Sr-isotope stratigraphy across the Lowe–Middle Cambrian

transition of the Cantabrian Mountain (Spain) and the Montagne Noire (France), West Gondwana. Palaeogeography, Palaeoclimatology, Palaeoecology 256, 47–70.
Yepifanov, V.A., 2012a. Galaxy pulsing, Earth space-time and the stratigraphic scale harmony. Geol. Mineralno-Syryevye Resursy Sibiri 4 (12), 90–103 (in Russian).
Yepifanov, V.A., 2012b. Geogalactic pulsations, space-and-time of the Earth and harmony of the stratigraphic scale. Discussionnye Voprosy i Gipotezy 4 (12), 90–103 (in Russian).
Zachos, J.C., Opdyke, B.N., Quinn, T.M., Jones, C.E., Halliday, A.N., 1999. Early Cenozoic glaciation, Antarctic weathering, and seawater $^{87}Sr/^{86}Sr$. Is there a link? Chemical Geology 161, 165–180.
Zakharov, Y.D., 1978. Rannetriasovye Ammonoidei Vostoka SSSR (Early Triassic Ammonoids of the East USSR). Izdatel'stvo "Nauka", Moscow (224 pp. (in Russian)).
Zakharov, Y.D., Naidin, D.P., Teiss, R.V., 1975. Oxygen isotope composition of Early Triassic cephalopod shells of Arctic Siberia and salinity of the boreal basins at the beginning of Mesozoic. Izvestiya Akademii Nauk SSSR, Seriya Geologicheskaya 4, 101–113 (in Russian).
Zakharov, Y.D., Vavilov, M.N., Popov, A.V., 1987. Shell microstructure of Late Palaeozoic and Triassic ammonoids of the Boreal realm. In: Zakharov, Y.D., Onoprienko, Y.I. (Eds.), Problemy Biostratigrafii Permi I Triasa SSSR (Problems of the Permian and Triassic Biostratigraphy of the East USSR). Far-Eastern Scientific Centre, USSR Academy of Sciences, Vladivostok (pp. 195–108 (in Russian)).
Zakharov, Y.D., Boriskina, N.G., Cherbadzhi, A.K., Popov, A.M., Kotlyar, G.V., 1999a. Main trends in Permo–Triassic shallow-water temperature changes: evidence from oxygen isotope and Ca-Mg ratio data. Albertiana 23, 11–22.
Zakharov, Y.D., Boriskina, N.G., Ignatyev, A.V., Tanabe, K., Shigeta, Y., Popov, A.M., Afanasyeva, T.B., Maeda, H., 1999b. Palaeotemperature curve for the Late Cretaceous of the northwestern circum-Pacific. Cretaceous Research 20, 685–997.
Zakharov, Y.D., Boriskina, N.G., Popov, A.M., 2001. Rekonstruktsiya uslovij morskoj sredy pozdnego paleozoya i mezozoya po izotopnym dannym (na primere severa Evrazii) (The Reconstruction of Late Palaeozoic and Mesozoic Marine Environments From Isotopic Data: Evidence from North Eurasia). Izdatel'stvo "Dalnauka", Vladivostok (112 pp. (in Russian)).
Zakharov, V.A., Baudin, F., Dzyuba, O.S., et al., 2005. Isotopic and faunal record of high paleotemperatures in the Kimmeridgian of the Subpolar Urals. Geologiya i Geophizika 4 (1), 3–20 (in Russian).
Zakharov, Y.D., Shigeta, Y., Smyshlyaeva, O.P., Popov, A.M., Ignatiev, A.V., 2006a. Relationship between $\delta^{13}C$ and $\delta^{18}O$ values of the recent nautilus and brachiopod shells in the wild and problem of reconstruction of fossil cephalopod habitat. Geosciences Journal 10, 325–338.
Zakharov, Y.D., Shigeta, Y., Tanabe, K., Iba, Y., Smyshlyaeva, O.P., Sokolova, E.A., Popov, A.M., Velivetskaya, T.A., Afanasyeva, T.B., 2006b. Campanian climatic change: isotopic evidence from Far East, North America, North Atlantic and Western Europe. Acta Geologica Sinica 81 (6), 1049–1069.
Zakharov, Y.D., Smyshlyaeva, O.P., Popov, A.M., Shigeta, Y., 2006c. Izotopnyj sostav pozdnemezozojskikh organogennykh karbonatov Dalnego Vostoka (stabilnye izotopy kisloroda i ugleroda, osnovnye paleoklimaticheskiye sobytiya i ikh globalnaya korrelyatsiya) (Isotopic Composition of Late Mesozoic Organogenic Carbonates of Far East (Oxygen and Carbon Isotopes, Palaeoclimatic Events and their Global Correlation)). Izdatel'stvo "Dalnauka", Vladivostok (204 pp. (in Russian)).
Zakharov, Y.D., Smyshlyaeva, O.P., Shigeta, Y., Popov, A.M., Zonova, T.D., 2006d. New data on isotopic composition of Jurassic – Early Cretaceous cephalopods. Progress in Natural Science 16 (Special Issue), 50–67.
Zakharov, Y.D., Sha, J., Popov, A.M., Safronov, P.P., Shorochova, S.A., Volynets, E.B., Biakov, A.S., Burago, V.I., Zimina, V.G., Konovalova, I.V., 2009. Permian to earliest Cretaceous climatic oscillations in the eastern Asian continental margin (Sikhote-Alin area), as indicated by fossils and isotope data. GFF 131, 25–47.
Zakharov, Y.D., Shigeta, Y., Smyshlyaeva, O.P., Popov, A.M., Velivetskaya, T.A., Afanasyeva, T.B., 2011. Cretaceous climatic oscillations in the Bering area, Alaska and Koryak Upland: isotope and palaeontological evidences. Sedimentary Geology 235, 122–131.
Zakharov, Y.D., Baraboshkin, E.Y., Weissert, H., Michailova, I.A., Smyshlyaeva, O.P., Safronov, P.P., 2013a. Late Barremian–early Aptian climate of the northern middle latitudes: stable isotope evidence from bivalve and cephalopod molluscs of the Russian Platform. Cretaceous Research 44, 183–201.
Zakharov, Y.D., Haggart, J.W., Beard, G., Safronov, P.P., 2013b. Late Cretaceous climatic trends and a positive carbon isotope excursion at the Santonian-Campanian boundary in British Columbia. Sedimentary Geology 295, 77–92.
Zakharov, Y.D., Tanabe, K., Shigeta, Y., Safronov, P.P., Smyshlyaeva, O.P., Dril, S.I., 2016. Early Albian marine environments in Madagascar: an integrated approach based on oxygen, carbon and strontium isotopic data. Cretaceous Research 58, 29–41.
Zakharov, Y.D., Horacek, M., Shigeta, Y., Popov, A.M., Maekawa, T., 2017. Carbon and nitrogen isotope record of Induan–Olenekian sequences in South Primorye and conditions for ammonoid and brachiopod recovery after Late Permian mass extinction. Doklady Earth Sciences. https://doi.org/10.1016/j.sedgeo.2017.11.01 (in press).
Zakharov, Y.D., Kakabadze, V.Z., Sharikadze, M.Z., Smyshlyaeva, O.P., Sobolev, E.S., Safronov, P.P., 2017a. The stable O- and C-isotope record of fossils from the upper Barremian–lower Albian of the Caucasus: palaeoenvironmental implications. Cretaceous Research 2017. https://doi.org/10.1016/j.cretres.2017.07.023.
Zakharov, Y.D., Seltser, V.B., Kakabadze, M., Smyshlyaeva, O.P., Safronov, P.P., 2017b. Isotope composition of Mesozoic mollusks from the Saratov-Samara region and main Early Cretaceous climate trends at the Russian Platform-Caucasus area. In: Same, B. (Ed.), 10th International Symposium on the Cretaceous (August 21–26 2017, Vienna – Abstracts). Berichte der Geologischen Bundesanstalt 120, p. 310.
Zhang, R.Y., Liou, J.G., Ernst, W.G., 2009. The Dabie-Sulu continental collision zone: a comprehensive review. Gondwana Research 16, 1–26 (in press).